



Label—Free Integrated Optical Biosensors for Multiplexed Analysis

Soumyo Mukherji^{1*} and Nirmal Punjabi²

Abstract | The need for real time, fast and frequent monitoring in health-care, pharmaceuticals research, environmental monitoring, the food industry, and homeland security has been rising, leading to extensive research in the development of Point of Care (POC) devices for diagnostics. POC devices need to be handy, fast, robust, highly sensitive to sensing analytes, selective against other interferents, and accurate. Since, in the real world scenario, the analytes are typically complex and useful analysis depends on sensing multiple parameters, multianalyte sensing has emerged to help users arrive at concrete conclusions or inferences. Research has been conducted for exploiting a plethora of transduction phenomena, such as electrochemical, impedometric, piezoelectric, magnetic, optical, *etc.* Of these, optical methods of sensing have the upper hand due to their resistance to electromagnetic interference, fast response, ease of parallel analyte sensing, low Limit of Detection (LOD), and, most importantly, easy translation of well-established techniques to *in silico* devices.

Label-free biosensing provides the advantage of simplicity and cost reduction by avoiding complex steps prior to sensing by monitoring analytes in their unmodified state i.e. detecting analytes without any alteration. Further, sensing in ultra-small quantities has been possible due to the concurrent development of MEMS technology. All this has led to the development of Lab on Chip (LOC) devices which perform various separation, and detection, operation and analysis on small chips and are cost effective due to bulk fabrication. LOC devices integrating label—free optical sensing on small chips also give rise to the possibility of multi-analyte assays using small test samples. These facilitate on-site deployment of these devices for different applications. This review will present various optical waveguide-based devices, including those based on optical absorbance, evanescent wave absorbance and surface plasmon resonance. Various configurations of such devices that aid multianalyte on-chip assays will be explored.

Keywords: *Integrated, Label free, Lab-on-chip, Multiplex, Optical Biosensor.*

1 Introduction

The need for the detection of various physical quantities like temperature, pressure, electromagnetic waves, light, current, *etc.* has led to the development of various techniques in the field of

physical sensors. Over the past century there has been significant progress in the development of chemical sensors as well. As may be easily surmised, physical and chemical sensors are distinguished on the basis of the measurand. Both types of sensors

¹WRCBB, Department of Biosciences and Bioengineering; Centre for Research in Nanotechnology and Sciences; Centre of Excellence in Nanoelectronics, IIT Bombay, Powai, Mumbai, India.
*mukherji@iitb.ac.in

²WRCBB, Department of Biosciences and Bioengineering, IIT Bombay, Powai, Mumbai, India.

Biosensors: are a group of sensors/analytical devices using biological molecules as receptors, in conjunction with various transduction techniques for effective sensing.

Analyte: is a substance/entity of interest to be analyzed or detected from a sample.

Integrated optical sensors: are types of optical sensors in which all the components are combined together on a single chip or substrate.

employ unique transduction phenomena in order to perform measurements. **Biosensors** on the other hand are sensors that employ biological recognition molecules and leverage on the physical/chemical transduction schemes of physical/chemical sensors, in order to qualitatively or quantitatively assess the measurand. Biosensors have gained tremendous importance ever since the first demonstration by Clark and Lyons¹ in 1962. They have the ability to detect **analytes** rapidly and precisely by using various biological molecules or biologically derived molecules like DNA,² peptides,³ cell structures,⁴ enzymes,⁵ antibodies,⁶ *etc.* as recognition elements, integrated or associated closely with different transducers. Based on the transduction principle used for sensing, biosensors may be grossly classified into electrochemical,⁷ optical⁸ and mechanical.⁹

Amongst the various types of biosensors, optical biosensors have emerged as the most popular. Most likely this is due to the fact that optical transduction is immune to electromagnetic interferences and mechanical vibrations. Further, quite a few of *in vitro* chemical and biological assays which had been developed earlier exhibit a change in optical properties on reaction. The translation of these chemical/biological assays to a biosensor format, so that minute changes in optical properties are detected, was a logical progression in terms of development. Optical biosensors, like other biosensors, can offer possibilities of multiplexing, real time measurements, low LOD, *etc.* Conventional optical biosensors relied on macro-scale instruments and devices; however, with the continuous development in microfabrication and micromachining technologies necessitated by ever-shrinking electronic devices, the possibility of shrinking the size of optical biosensor devices as well emerges. This has, in turn, reduced the volume

requirement of reagents, and analytes and brought forth the possibility of making multiple measurements using the same physical device or devices arranged within a few microns of each other.

In the early days of optical biosensor development, a large number of sensors and sensing systems relied on labeled assays or tagged assays. In these assays, typically, a capture or recognition event by a biomolecule was followed by a signal enhancement/amplification step using a probe molecule “tagged” or “labeled” with an enzyme, fluorescent marker, radioisotope, *etc.* In some cases, the probe molecule itself exhibited fluorescence or other signal amplification behavior. However, these assays obviously had a disadvantage in terms of the complexity of the measurement process. Along with the development in transduction technologies and science, it became possible to detect a change in optical properties without the application of a tag. Thus, in parallel with the development of optical microsensors, researchers also targeted the development of label free assays, which can significantly reduce the cost and complexity of the measurement in the hands of the user. The high degree of interest in developing label-free sensing technologies has resulted in a large number of publications in this domain (Figure 1). The increase in the number of publications which deal with the development of “label free biosensors” has been 50-fold over the last decade. Further, in 2011, amongst the publications related to sensors, about 53% dealt with optical sensors (Figure 2).

In recent years, optical biosensors have found a wide range of application in various fields like proteomics,¹⁰ biomedical research,¹¹ biological interaction: to measure both kinetic and thermodynamic parameters of the interaction,¹² pharmaceuticals/drug discovery,¹³ clinical diagnostics,¹⁴ environmental

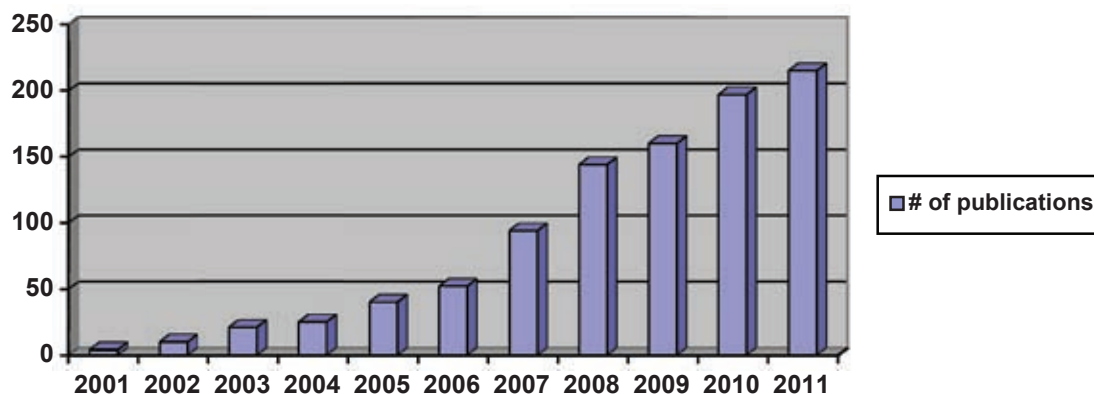


Figure 1: Number of publications involving the concept of “Label free biosensors”.
Source: ISI Web of Knowledge.

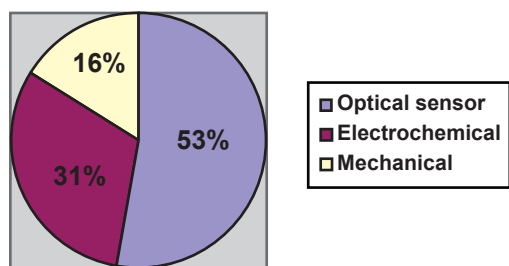


Figure 2: Publications on different types of sensors in the year 2011.
Source: ISI Web of Knowledge.

monitoring,¹⁵ combinatorial libraries,¹⁶ food safety,¹⁷ security,¹⁸ *etc.*

This review aims at exploring the translation of large, macro-scale devices to miniaturized devices fully capable of analyzing a sample for more than one biological/chemical measurand. To this order, the review will initially discuss the various methods, phenomena and instruments adopted for developing optical biosensors. Thereafter, the research performed towards the integration of such devices on microfabricated chips and the creation of multiple sensors, contiguous to each other by various research groups will be discussed.

2 Biosensors, an Introduction

Biosensors are sensors that utilize a biologically derived species (molecule, cell, *etc.*) in close proximity to or contiguous to a physical or chemical transduction mechanism in order to create a reagentless (between the biological species and the transducer) system for the detection of an analyte. Biosensors can be classified according to the type of transduction mechanism, the transduction platform, the recognition mechanism or the analyte to be detected. Optical biosensors, a type classified on the basis of the transduction platform/mechanism, form an elite group of biosensors, which have been widely researched and commercialized. It is still one of the most hotly researched areas.

The scheme of a typical biosensor is given in Figure 3 and the gross mechanism of the functioning of a biosensor in Figure 4.

As can be seen from Figure 4, if the sensing action, or a measurable output signal, can be derived at step 3, reporter molecules, tagged with “labels”, are not required, thereby eliminating a step in the measurement process and reducing complexity and the time consumed in measurement. Such measurements are termed “label free” and are at present one of the primary foci in biosensor research.

Biosensors are classified as labeled if the sensing element (or secondary sensing element, as in

the case of sandwiched assays)¹⁹ is tagged with radioisotopes,²⁰ fluorescent dyes,²¹ semiconductor quantum dots,²² *etc.* or as label-free if the sensing element is not tagged. **Labeled biosensors** have been used for quite a long time as they provide low LOD, ease of availability of instruments for sensing and optimized/standardized labeling procedures. However all these advantages of labeled sensing are not able to overcome the effect of problems faced due to labeling in various applications.^{23,24} The labeling procedure is time-consuming; due to the addition of extra steps, labeling has a higher operation cost. As additional reagents are required, labeling cannot be used for real time monitoring of analyte binding; and can interfere with analyte binding. Labelling also poses a difficulty in multiplex analysis due to the need of different labels leading to further complex procedures. Also, different tags have their inherent problems such as: 1) In the case of radioisotopes: short lifetime, high cost, generation of a large quantity of hazardous contaminants and the need for sophisticated hot labs and 2) In the case of fluorophores: excitation and emission efficiency is reduced with usage by photobleaching and loss of kinetic information as the assay is read at the end to avoid interference by light²⁵ Also quenching and self-quenching reduces the efficacy of tags in a stochastic way. Also some of the tags are not compatible with live cells, so the same sample cannot be studied again.

These problems, along with the need for inexpensive, user friendly, POC devices, have led people in industry and research institutions to move towards their counterpart: label-free sensing.²⁶ Label-free sensing is relatively less expensive and reduces testing time. The sensitivity of label-free sensors was a concern; however, with advancements in transducer technology this problem has been largely overcome. These sensors also perform real time studies as they measure the inherent property of the analyte to be detected. This reduces the experimental uncertainty caused due to interference by the label. Based on these advantages, label-free sensing leveraging on transduction techniques like Surface Plasmon Resonance (SPR), Interferometer, *etc.*, has found applications in various fields.

Label-free sensing can be classified as direct or indirect. In direct assays, the response is directly proportional to the amount of analyte present. Direct label free sensing is a simple, one step, and reagentless operation.²⁷ However, direct assays may not always be ideally suited for a particular detection. In such cases, an indirect assay is used, where the binding reaction between a capture molecule immobilized on the sensor surface

Labeled biosensors: are biosensors using tags/labels along with transduction techniques to improve efficacy of detection.

Label-free biosensors: are biosensors using transduction principles for the direct detection of analytes.

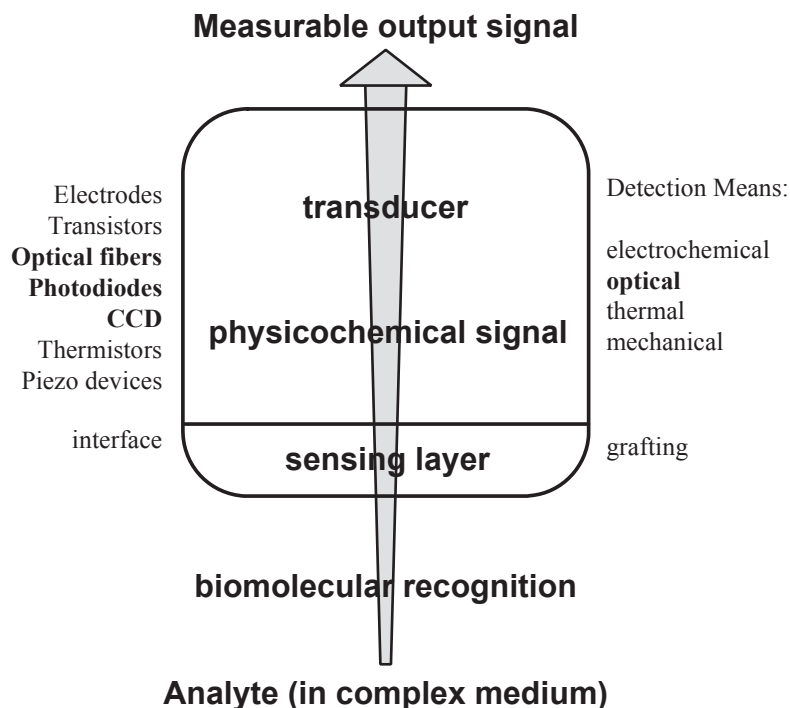


Figure 3: Schematic of a biosensor.

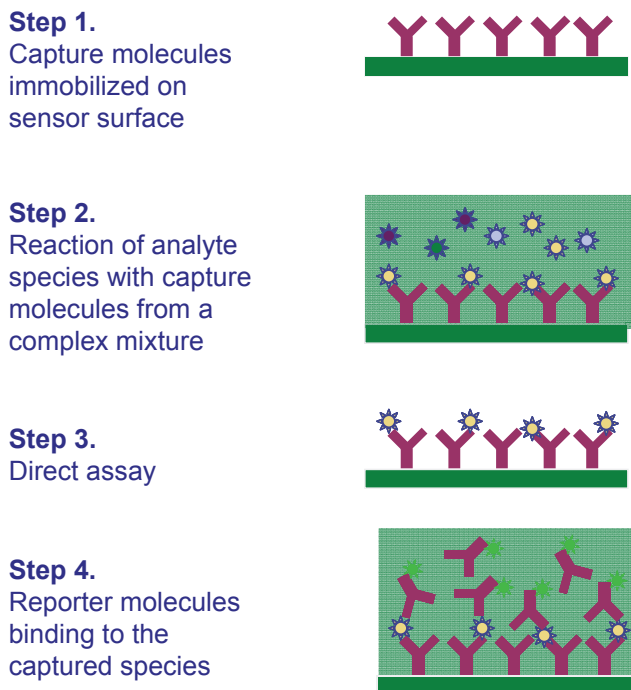


Figure 4: Direct assay and labeled assay.

and a pre-assigned complementary molecule (or species) is inhibited by the presence of the target measurand.

As mentioned earlier, optical sensing has gained tremendous importance due to its inherent

advantages over other transduction mechanisms. Optical sensors can work along with both labeled and label free formats. Label free optical sensing usually induces a change in the amplitude, phase, polarization, or frequency of input light in response

to a physical or chemical change produced at the sensing surface. These changes in the light signal are usually related to small changes in the refractive index or absorbance due to the presence of the analyte to be detected in the proximity of the sensor. Different combination of materials and their concentrations may have a similar change in the refractive index leading to possible ambiguity in the case of complex analytes. Therefore, to make the sensing process specific/selective, a receptor molecule, which is specific for a particular analyte, has to be immobilized on the sensor surface. The binding of biomolecules will cause a change in the optical properties at the surface of the sensor and thus can be calibrated to predict the concentration.

One of the primary issues that researchers in the field of optical biosensors face, is the fact that simple optical transmission (or absorption) based detection systems, where light passes through the analyte volume, are frequently plagued by inaccuracies due to multiple interfering species in the analyte volume. Therefore the issue of light coupling into the system assumes crucial importance. The key to this lies in the use of the interaction of the evanescent wave with the biomolecule of interest. In this regard, a short discussion on the origin and properties of the evanescent wave may not be out of order.

When light is coupled into a material and the ray of light strikes at angle θ_i at the interface of two non-absorbing structures having refractive indices n_i and n_r ($n_i > n_r$), some part of the light is refracted and the remaining is reflected back as seen in Figure 5a. At the critical angle θ_c light is propagated at the surface as seen in Figure 5b. When incident angle $\theta_i > \theta_c$, light is reflected back totally as seen in Figure 5c. This phenomenon is

known as total internal reflection (TIR) and the wave is termed a 'guided wave'. In such cases, at the junction, there is no net transfer of energy. However, the boundary condition cannot be zero. This leads to the formation of an evanescent wave, whose power decreases along with the distance from the surface.

The evanescent wave is formed at the surface of all the waveguides and can be exploited for use in biosensors. It is also particularly advantageous since the light in this case never actually passes through the analyte volume and is therefore relatively uncorrupted by interfering species. We will illustrate the concept of evanescent wave (EW) based sensing using optical fiber sensors, while explaining/mentioning the EW based sensing that has been successfully exploited in many other formats.

2.1 Evanescent wave-based sensing on optical fibers

The structure of an optical fiber is shown in Figure 6. The region in which light is coupled and hits the junction of two surfaces is termed as the 'core', whose refractive index is greater than the cladding. Since light is coupled in such a fashion that the angle of incidence at the core-cladding interface is more than the critical angle, light propagates, virtually undiminished through an optical fiber. This has led to a revolution in communication technologies in the last fifty years. A careful analysis of the core-cladding interface reveals an evanescent field as the tail of the bell shaped field of the guided wave. The penetration and absorption of the evanescent wave is affected by the relative refractive indices of the core and its surroundings, the wavelength of light, *etc.* If the jacket and cladding are removed, leaving only the

Waveguides: are structures guiding electromagnetic waves using the principle of Total internal reflection.

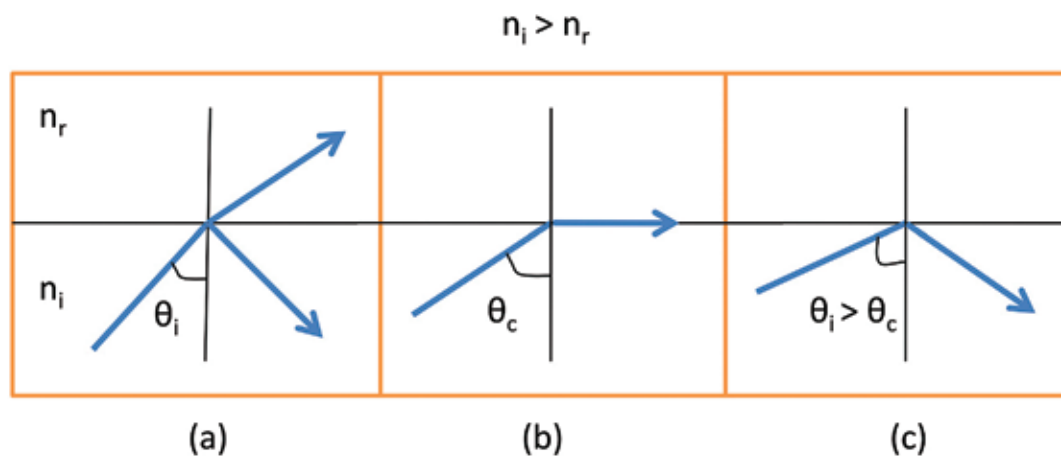


Figure 5: Illustrations of total internal reflection.

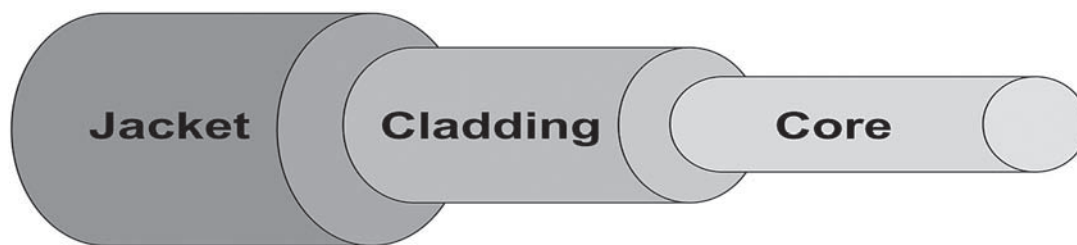


Figure 6: Basic structure of optical fiber.

core, the evanescent wave can be seen penetrating into the medium surrounding the core. In case biological molecules are immobilized on the surface of the core, the evanescent wave will be affected not only by such molecules but also target molecules that may bind to the immobilized capture molecules.

Of particular interest is the fact that the penetration depth (d_p) of the evanescent wave (defined as the distance at which the magnitude of the electric field at the surface decays to its $1/e$ value) and given by Eq. (1),²⁸ is very small, effectively of the order of a few hundred nanometers for straight fibers. Therefore, interfering species beyond this distance hardly affect the field of the propagating light.

$$d_p = \frac{\lambda}{2\pi \cdot n_{co} \sqrt{\left(\sin^2 \theta - \frac{n_{cd}^2}{n_{co}^2}\right)}} \quad (1)$$

where λ is the wavelength of the incident light, θ is the angle of incidence, n_{co} and n_{cd} are the refractive index of the core and cladding, respectively.

Straight and cylindrical optical fibers provide good sensitivity and low loss. However, due to the low effective depth of penetration of the evanescent wave they are not sensitive towards target species which have a size beyond a few tens of nanometers. So, it is difficult to detect cells, which usually have sizes ranging beyond a few hundred nanometers. It has been theoretically proven, and practically demonstrated, that changing the design or geometry of optical fiber probes can increase the depth of penetration of the evanescent waves.²⁹ U-bend and tapered probes have been used by many researchers in order to increase the sensitivity of fiber probes.^{30,31}

Bharadwaj *et al.*, 2011 had demonstrated evanescent wave absorbance based sensing using U-bent optical fibers for label-free detection of *E. coli* by measuring change in absorbance at 280 nm. A schematic depicting the relative advantage of a bent fiber over a straight fiber, with respect to evanescent power and depth at the sensing surface, is shown in Figure 7.³² For the

purpose of sensing, the U-bend part is decladded in the bend region. The depth of penetration of the evanescent wave in the bend part increases to an extent that the evanescent wave can effectively be affected by bacteria cells. The binding of *E. coli* cells to the antibodies immobilized on the surface increases the absorption of the electromagnetic wave (UV light) propagating through the fiber, due to the absorption of 280 nm wavelength of light by proteins in and on the bacterial cell.

The evanescent wave is utilized for sensing in many other devices due to the advantages mentioned earlier. Some of the most prominent ones of these are those which utilize the interaction of the evanescent field with the surface plasmons in a metal-dielectric interface.

2.2 Surface Plasmon Resonance (SPR) based devices

Extensive research has gone into the field of SPR biosensing, right from the time it was first demonstrated for such a purpose by Liedberg *et al.*, in 1983.³³ At present, a large number of papers discussing optical biosensing are based on the principle of SPR. A surface plasmon wave (SPW) is a charge density oscillation occurring due to the interaction of light photons with free electrons at a metal dielectric interface. At specific resonant wavelengths, the energy of the incident photons is transferred to the free electrons on the metal surface, leading to the phenomenon of Surface Plasmon Resonance. The power of the surface plasmon wave decreases exponentially in the direction perpendicular to the surface. The wavelength of light at which SPR occurs depends critically on the refractive indices of the dielectrics on the two sides of the metal and the metal itself. Assuming that the medium on one side of the metal film and the film itself are fixed for coupling the light photons in, the primary determinant of the resonance frequency will then be the refractive index of the medium on the other side of the metal film and the angle (greater than the critical angle) of incidence of the light photons. On the other hand, if the wavelength of light being incident on the interface

SPR: is a resonant oscillation of valence electrons in a metal due to the transfer of energy of incident light at resonance condition, which is dependent on the refractive index, wavelength, incident angle and surface material.

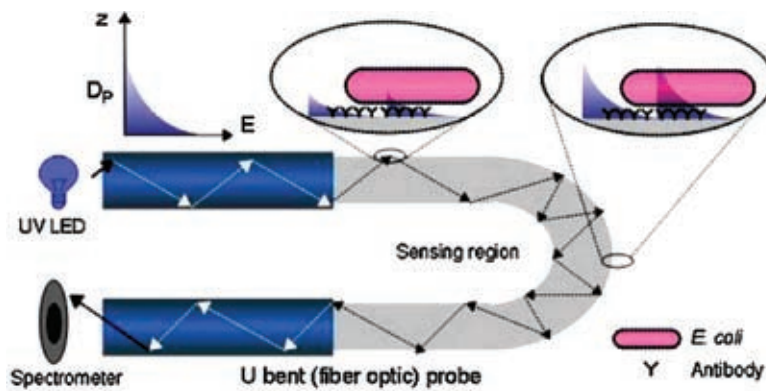


Figure 7: Enhancement of penetration depth ' D_p ' in a bend fiber probe, enabling evanescent field overlap for the detection of *E. coli*.³²

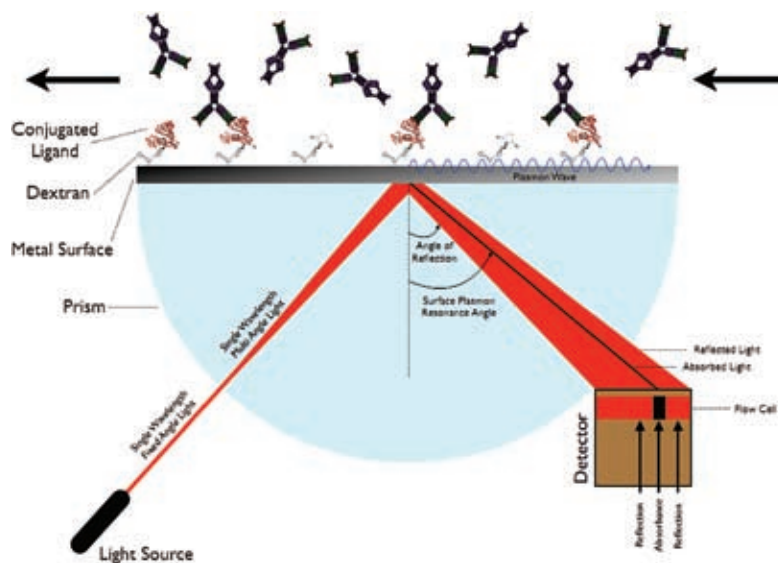


Figure 8: Schematic of SPR sensing.³⁷

is fixed, then the angle at which resonance occurs will be determined by the refractive index of the aforementioned medium. Both of these are very sensitive to minute changes in RI and thus can be utilized to study the biomolecular binding that affects the refractive index of the medium near the interface. SPR devices conform to three common configurations, namely, the Prism coupled based SPR system,³⁴ the waveguide based SPR system,³⁵ and the Grating coupler based SPR system.³⁶ The Prism coupled based SPR system is the most commonly used configuration. A schematic of SPR sensing using prism coupled is shown in Figure 8.

2.3 Localized Surface Plasmon Resonance (LSPR) based sensors

Localized surface plasmons are charge density oscillations confined to around metal nanoparticles

or nanostructures³⁸ as shown in Figure 9. This phenomenon, like SPR, is created due to light of a particular wavelength incident on an assemblage of dispersed nanoparticles or distinct nanostructures. The wavelength of light at which LSPR is observed therefore depends on the material, the size and shape of the nanoparticles or structures as well as the refractive index of the medium immediately around them. Like evanescent waves, the intensity of the oscillations decays along with the distance from the surface of the nanoparticles. LSPR based sensors have been in existence for a very long time and they have been used in various formats starting from dispersed nanoparticles in solution, to color changing strips and, more recently, nanoparticles immobilized on optical fibers⁶ or waveguides.³⁹ More details regarding the use of such nanostructures and films can be found in the review written by Satija *et al.*⁴⁰

LSPR: is surface plasmons generated in the vicinity of nanoparticles whose dimensions are less than the wavelength of incident light.

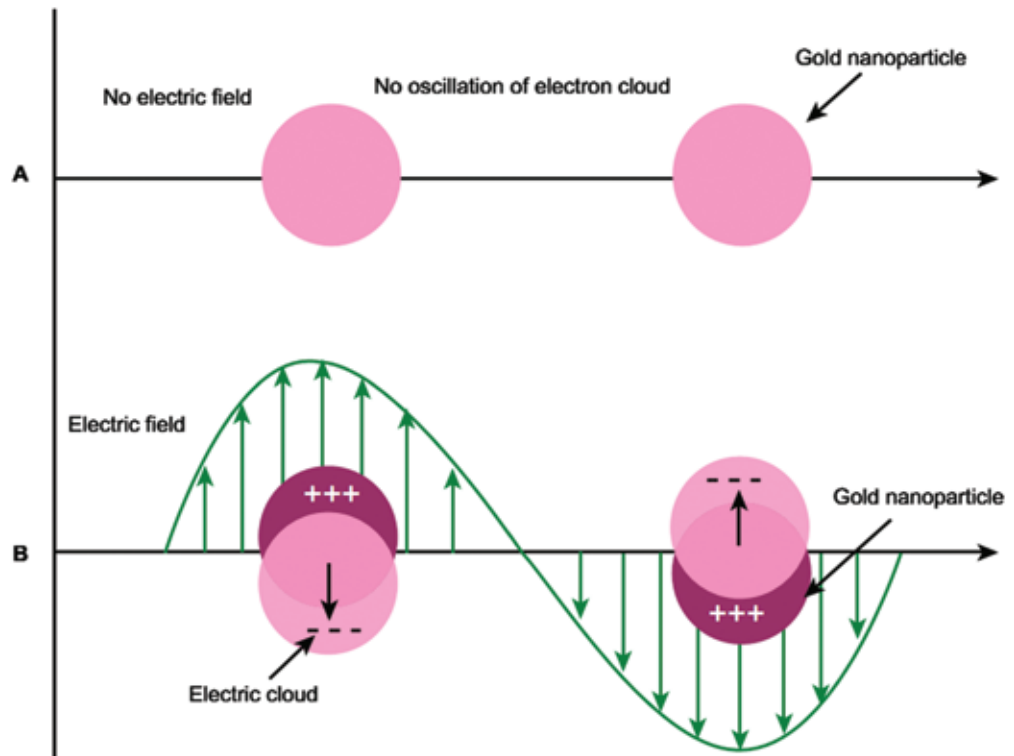


Figure 9: Schematic of LSPR generation in the vicinity of a nanoparticle.⁴⁰

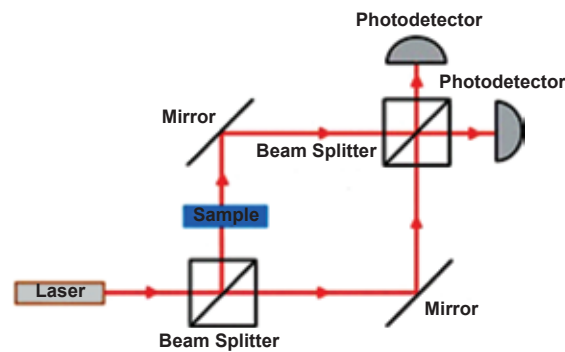


Figure 10: Free space schematic of a Mach-Zehnder interferometer.⁴¹

2.4 Interferometry-based devices

The change in refractive index due to the binding of an analyte has also been exploited in interferometry based devices. These devices depend on the physical phenomenon that a refractive index change in a medium participating in the transmission of light leads to a change of phase in the transmitted electromagnetic wave. This, if allowed to interact with a reference wave (which is not subject to a refractive index change in its path), will produce an interference pattern. The pattern depends obviously, amongst other things, on the change in RI, which makes it amenable to be used

as a biosensor. The simplest configuration of an interferometry-based device is the Mach-Zehnder interferometer (Figure 10), where a light beam is split into two parts which pass through reference and sensing waveguides and finally meet at a junction where they interfere and produce a characteristic pattern on a linear array optical detector.

The phenomenon of interference has also been used in a slightly different format where rays reflected from the interface between various layers in a composite layered structure interfere and produce a pattern. It is quite obvious that the change in refractive index of one of the layers

(most frequently the uppermost one) will shift the interference pattern. This technique has been named Reflectometric interference spectroscopy (RIFS). White light is partially reflected and transmitted at the interface of thin transparent layers with negligible absorption. If the optical pathlength is smaller than the coherence wavelength of incident light, then the different reflected partial waves of the incident wave interfere as seen in Figure 11. This leads to the formation of an interference pattern (constructive or destructive) which is dependent on the wavelength, incident angle, optical thickness (optical thickness is defined as product of physical thickness and the refractive index of the layer) and the refractive index of the uppermost medium. The binding of an analyte molecule or particle to the sensor surface causes a shift of the interference pattern in the wavelength axis.

2.5 Ellipsometry based devices

As mentioned earlier, the primary optical changes that can occur with a receptor target interaction is a change in the refractive index of the nano or micro environment and a change in the optical

absorption or extinction coefficient. A conventional and age-old technique called Ellipsometry, which exploits these changes has been adopted for use by many researchers for biosensing applications.^{43–45} Ellipsometry is based on the alteration in the polarization state of the reflected light due to changes in the dielectric property or refractive index of a sample surface. The foundation for this was laid by P. Drude in the late 1880s in a series of papers.⁴⁶ Drude used the reflection of polarized light for measuring the optical constants of metals. With the development of semiconductor microelectronics, and the need for measuring thickness in microns, this technique became very popular and is still used routinely in microfabrication facilities.

Measurements using ellipsometry are based on measuring the optical constants of the material which depend on the refractive index and extinction coefficients. Figure 12 shows that the schematic of measurement, where linearly polarized light on reflection from a surface, becomes elliptically polarized. The eccentricity and the orientation of the axis of the ellipse are dependent on the angle of incidence and optical properties of the surface. Ellipsometric

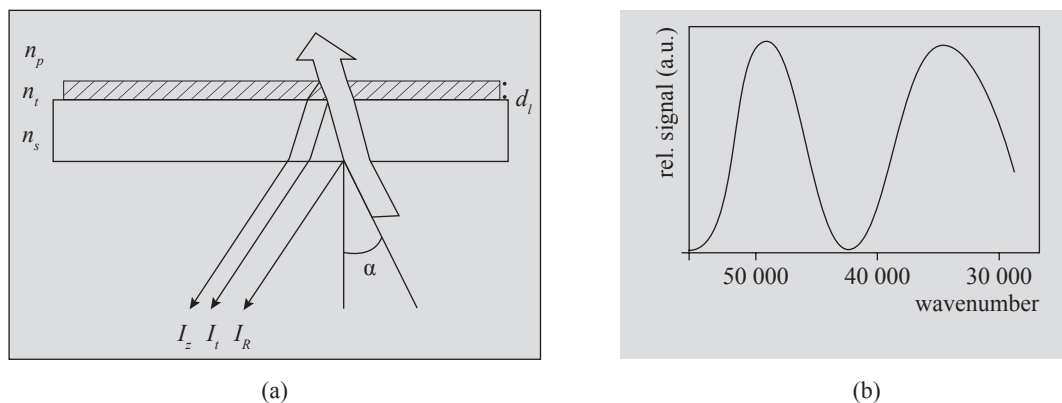


Figure 11: Principle of RIFS sensing (a) Schematic; (b) Corresponding interference pattern.⁴²

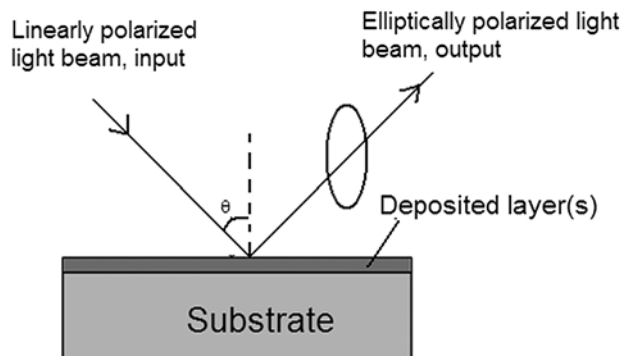


Figure 12: Schematic of principle of measurements using ellipsometry.

parameters i.e. the amplitude parameter (ψ) and phase parameter (Δ) derived from the output allows modeling the reflection coefficients which depend on the optical properties of the material, along with optical parameters like wavelength and angle of incidence of the input light. The two parameter measurements increase the accuracy and thereby the usability of ellipsometric measurements for the characterization of thin films.

One of the main limitations of conventional ellipsometry is that the light beam passes through the medium under study. This affects the use of this technique in real biosensing applications, as species other than the target may affect the output. Further, the sensitivity may also depend on the nature of the solid-liquid interface and be lower than solid-solid interfaces. Conventional ellipsometry has poor sensitivity for different solid liquid interfaces. To overcome the disadvantages, a modification of conventional ellipsometry known as Total Internal Reflection Ellipsometry (TIRE) or surface plasmon enhanced ellipsometry⁴⁷ has been developed.

It was reported that phase modulated ellipsometry can detect different phase transitions in the monolayers of surfactants on water.⁴⁸ This was backed by Kim *et al.*, 1989⁴⁹ by using ellipsometry based on TIR, as in the SPR devices of the Kretschmann configuration, combined with ellipsometry of the reflected light. The schematic of TIRE is shown in Figure 13. The setup is similar to conventional ellipsometry, except for the addition of a prism along with the glass slide coated with a thin metal film. Polarized light enters the prism, undergoes TIR at the glass metal interface, and causes SPR at the metal surface when resonance conditions are fulfilled. SPR causes minima in the

reflectivity vs. angle plot. A change in the surface characteristics of the metal layer (due to biological or chemical interactions) changes not only the position of the minima but also the phase of the reflected light. The specialty of TIRE is that it has the advantages of both SPR i.e. the light beam does not pass through the sample medium and is highly sensitive to refractive index coupling during weak coupling⁵⁰ and Ellipsometry i.e. it detects both amplitude variations and phase variations. It has been reported that TIRE is 10 times better than conventional SPR.⁵¹

2.6 Ring resonator

Ring resonators are based on a concept analogous to “whispering galleries”. In these devices, there is a change in resonant wavelength due to a change in refractive index in the proximity of the resonating structure. In the setup of a Ring Resonator, a bus waveguide is kept adjacent to a circular (microring) waveguide structure (Figure 14) to couple light into the circular waveguide. Light of a particular wavelength will be coupled from the bus waveguide to the ring if it satisfies the resonant conditions given by Eq. (2):

$$n_{\text{eff}}L = m\lambda \quad (2)$$

where n_{eff} is the effective refractive index of the ring which depends on immobilized biomolecules, analytes near the surface and bulk refractive index; L is the circumference of the ring; m is an integer; and λ is the wavelength. Ring resonator-based sensing is dependent on the quality factor. If the quality factor is high, then the resonance peaks become narrow, which facilitates the detection of

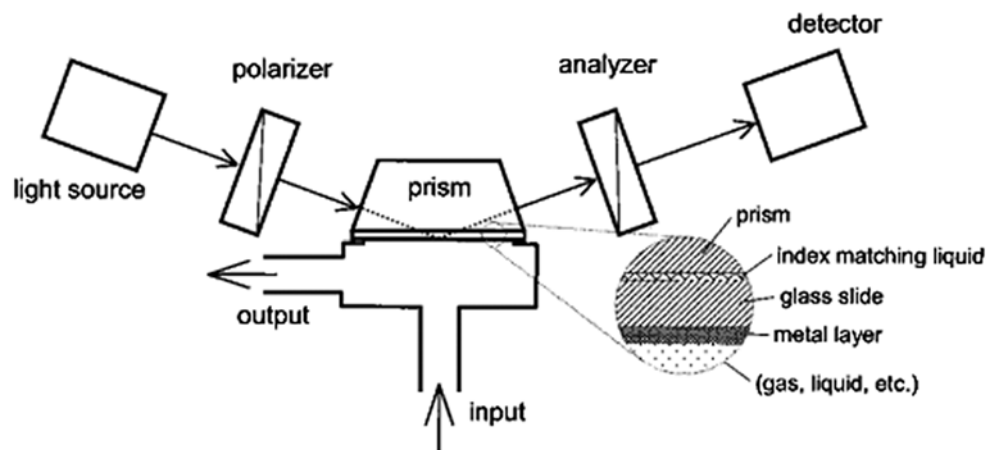


Figure 13: Schematic of TIRE. Magnification shows different stacks of layers between the flow cell and prism.⁵¹

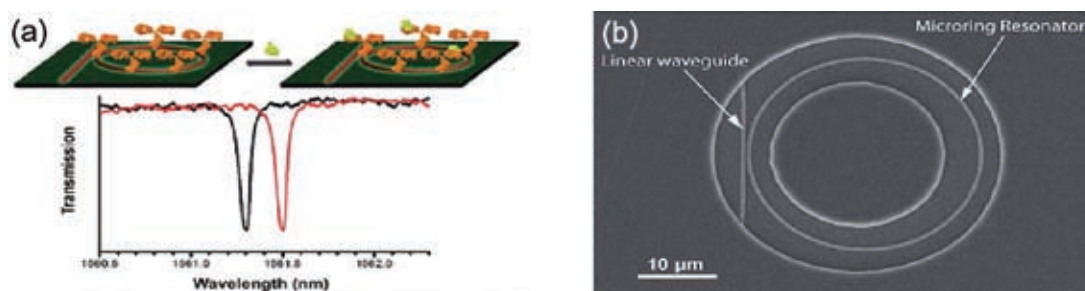


Figure 14: Micro Ring Resonator: (a) Working; (b) Top view of microring with adjacent waveguide.⁴¹

small shifts, thereby increasing spectral resolution. When the biomolecular capture agent is immobilized on the ring, a particular resonant peak is observed based on the effective refractive index. If there is a binding of the analyte with the capture agent, there is a change of the effective refractive index which changes the resonant condition and thereby causes a shift in the resonant wavelength as shown in Figure 14(a).

Most of the devices described in the preceding sections were developed relying on either large external instrumentation systems and/or large sensor devices. This makes them difficult to use in point-of-care applications and in detecting multiple analytes from a small sample volume. However, with the development of microfabrication, MEMS and MOEMS technologies, it is entirely possible to integrate these devices on a chip with minimal external instrumentation. Further, in the process of integration and miniaturization, it is also entirely possible to put multiple sensing heads on the same chip and essentially detect more than one target analyte in a sample. The following sections describe research and development efforts from laboratories worldwide in creating integrated and multiplexed sensing systems based on the principles of the devices described earlier.

3 Integration and Miniaturization

The emergence and prevalence of a large number of infective and pathological diseases, and the discovery of biological markers identifying the diseases and sometimes the causative organisms, coupled to the large population in India and other emerging economies, has brought about the requirement of high scale integration and multiplexing in biosensors and devices. This also has led to the possibility of Point of Care (POC) devices, which can perform the detection/testing decentralized either at the physician's office or at a patient's place.^{52,53} The first step towards such devices is the miniaturization of existing devices to perform sampling, detection, analyzing, *etc.* on a chip.

This section discusses some such efforts which can lead to multiplexed sensor applications which are discussed in a future section.

3.1 Evanescent wave absorbance based sensing using miniaturized optical waveguides

The requirement for on-chip optical communication has led to the development of on-chip optical waveguides. The structure of these waveguides is similar to optical fibers as seen in Figure 15. There is a high refractive index core sandwiched between two layers of low refractive index. The bottom layer is typically the substrate (silicon or an oxidized layer of silicon) and the top layer or "cover", is a deposited layer with a low refractive index, typically sputtered oxide or polymers. In the case of sensing applications, the cover is typically modified either physically or chemically. In the latter case, the cover layer is modified for selectivity towards a target by attaching receptor molecules. As in optical fibers, the evanescent wave generated at the interface is used for sensing. One of the main advantages of integrated waveguides is the ease of fabricating different probe geometries. Further, in the case of integrated waveguides, there is control over the dimensions of the waveguides down to sub-micron levels using fabrication technologies like E-beam lithography,⁵⁴ LIGA,⁵⁵ *etc.*

Prabhakar and Mukherji, 2010 have reported the fabrication of integrated polymer waveguides coupled with microfluidic channels using an SU-8 polymer. They have also reported the optimization of probe geometry and the dimension waveguides for higher sensitivity. U-shaped waveguides, along with the fiber couplers and microchannels were fabricated using single step SU-8 patterning. Figure 16(a) shows the image of a mask design for fabrication. The serpentine design helps in fabricating many waveguides together on the chip. The close-up in Figure 16(b) shows the microchannel having the U-bend area as one of the wall. Light from the source was coupled to the waveguide

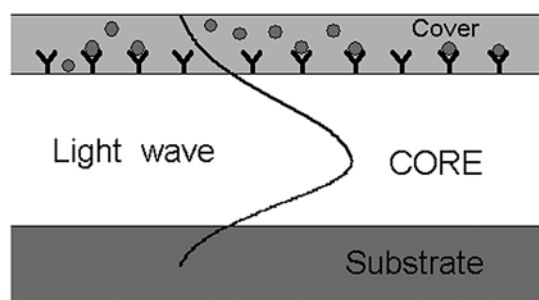


Figure 15: Evanescent field propagating in a waveguide.

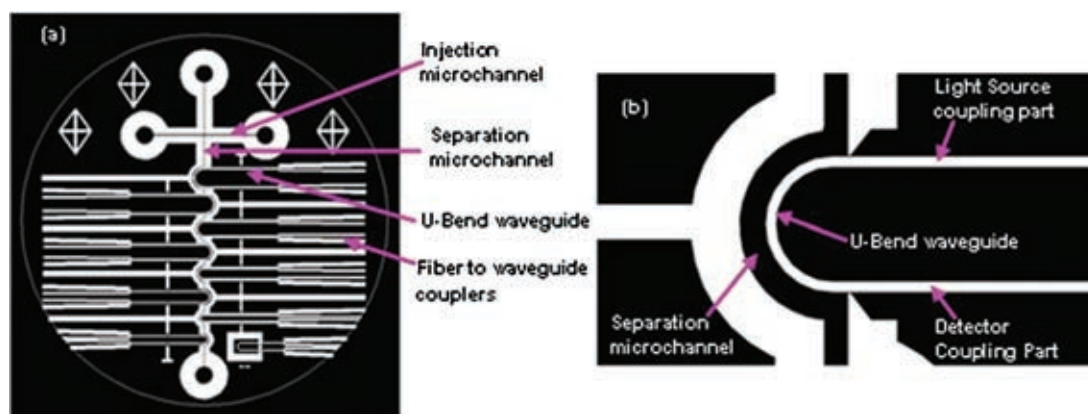


Figure 16: (a) Mask design of the U-bend waveguide; (b) Close-up of a U-bend waveguide.⁵⁶

using an intermediate optical fiber that is inserted into the waveguide-fiber coupler structure. The sensitivity of the waveguide was tested using different concentrations of Methylene blue and sucrose solutions.⁵⁶

3.2 Miniaturized SPR based biosensors

The possibility of exploring the SPR phenomenon using optical fibers has been looked into by many research groups around the world for quite a while, more so since optical fiber based SPR sensors may be able to dispense with the prism for the coupling optics. The primitive fiber optic-based SPR sensors had tips coated with a metal layer,⁵⁷ side coated,⁵⁸ cladding partly removed and metal deposited,⁵⁹ metal on taper,⁶⁰ etc. A particularly interesting device has been demonstrated by Kurihara *et al.*, 2004, who fabricated a fiber optic-based SPR microsensors by using selective chemical etching (SCE) technology.⁶¹ A microprism was created by selective chemical etching on the flat end of an optical fiber and a metal layer was sputtered on it. Figure 17(a) shows a micrograph of a microprism on an optical fiber. Figure 17(b) shows a further close up of the microprism having a base of approximately 1 μ m. Figure 17(c)

shows a schematic of the generation of surface plasmons on top of the metal coated microprism. When linearly polarized light is incident at the metal surface, surface plasmon waves are generated. These surface plasmons are dependent on the refractive index of the medium surrounding the SPR probe, the wavelength of light incident on the metal surface and the angle of the prism cone. Light reflected from the metallic surface of the microprism acts as an SPR signal. Figure 17(d) shows the optical system used to measure the shift in resonance spectra. Light from the optical source falls on the linear polarizer and through a beam splitter enters the single-mode optical fiber. The reflected light propagates through the fiber to the beam splitter and is directed towards the analyzer. The polarizers help separate the SPR signal from the input laser light. The cone angle can be modulated to define the refractive index range to which the SPR is sensitive. It has been reported that SPR in near infrared regions (NIR) shows more than thirteen times improvement in sensitivity.⁶²

The integration of the SPR phenomenon with optical fibers to reduce reagent and analyte volume requirements as well as to provide the possibility of multi-analyte sensing has also been attempted

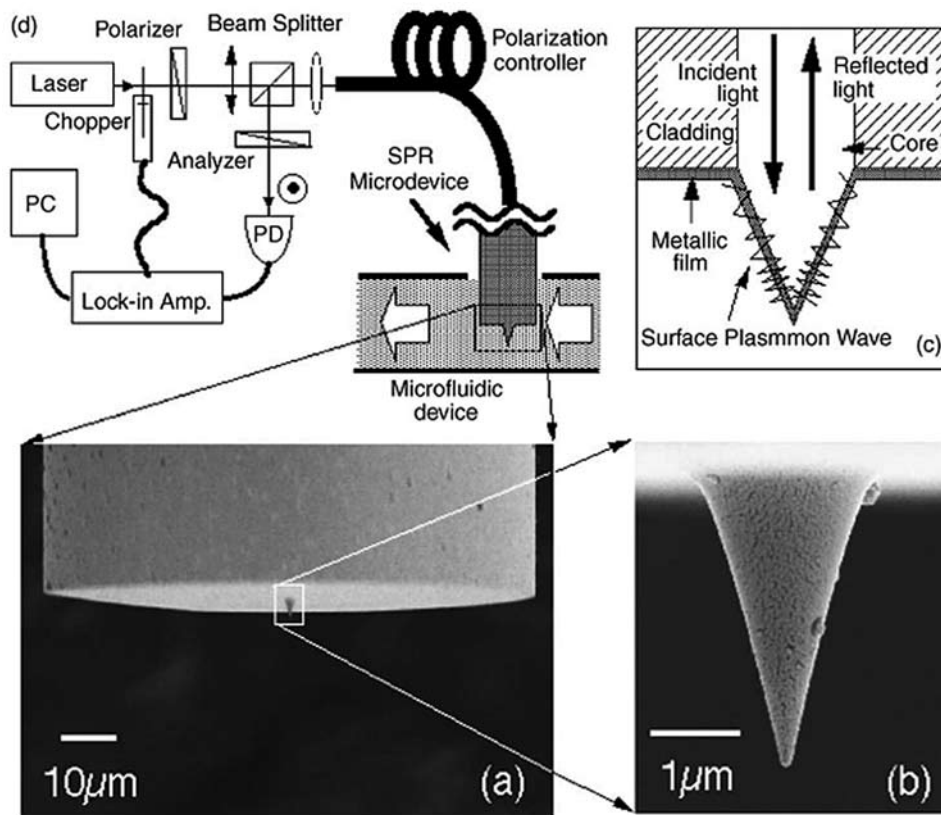


Figure 17: (a) Microprism fabricated using SCE; (b) Close up of microprism; (c) Generation of surface plasmon wave on the surface of metallic film on top of microprism surface; (d) Schematic of complete device.⁶¹

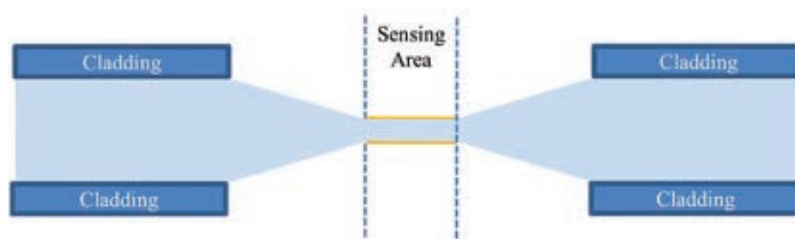


Figure 18: Cross-sectional drawing of a biconical tapered waveguide.

with tapered optical probes. The drawing of the design is shown in Figure 18, which is essentially a bi-conical taper with a straight neck used as the sensing region. This has shown better sensitivity in comparison to straight optical fiber-SPR probes. However, the taper ratio requires optimization since there is a maxima in terms of sensitivity.³¹ This design has been modified by the introduction of a layer of Teflon between the dielectric core and the metal surface.⁶³ This caused the formation of two SP waves on the two interfaces of the metal providing a sensitivity 15 times better than the conventional uniform core fiber. A further level of

miniaturization and integration in terms of using metal-coated tapers for optical fiber-SPR has been demonstrated by Srivastava and Gupta, 2011.⁶⁴ In this case, there are multiple tapers in series with taper periods short enough to increase sensitivity. The waveguide is within the flow cell so as to be used for sensing applications. It was observed that with a decrease in the taper period, the shift in spectra increases but the accuracy decreases due to the broadening of the spectra.

Although the reduction of the SPR devices to optical fiber based ones from the prism and glass slide based ones represent a considerable degree

of miniaturization and possible integration, there are many issues that plague fiber based sensors and make their possible use in POC devices doubtful. The principal amongst these relates to the diameter of the fiber. Since the sensitivity is expected to be higher with lower diameter fibers, the sensors should be made of very thin fibers. However, that adds to problems due to fragility and difficulties faced during alignment for light coupling. These problems can be reduced by adopting the same principles and designing on-chip waveguides, which can be easily fabricated with small dimensions, fewer dimensional errors and suitable coupler structures.

Different bulk components have been integrated on chips to miniaturize the setup and reduce loss due to external coupling.^{65,66} However, sensitivity and practicality issues have sometimes dictated only partial integration of the device, viz. integration of a select few of the individual components.

There is an elaborate review by Hoa *et al.*, 2007 giving insights about the change caused by integration on SPR.⁶⁷ The components involved in the basic SPR setup are the light source, optics like prisms and focusing lenses, a microfluidic system for controlling sample flow, a detector and supporting electronics and data analysis software to interpret the result. Also, the surface chemistry has an impact on the sensitivity of SPR. Light sources are shifting towards low power, stable, compact LED⁶⁸ and sophisticated laser sources.⁶⁹ One of the first integrated SPR sensors was Spreeta by Texas Instruments in 1996 which is currently owned by Sensata Technologies.⁷⁰ The Spreeta SPR is shown in Figure 19. The novelty in this miniaturized

setup is that the source, detector and electronics are encapsulated in the optical covering thus making it compact.

The light path is from a AlGaAs (Aluminum Gallium Arsenide) LED source, followed by a polarizer. The polarized light then falls on the SPR chip with a limited range of incidence angles and the output light falls on the mirror, which reflects it to a sensitive linear photodiode array. Each pixel of the detector generates an output corresponding to a small range of incident angles. All the components are enclosed by shielding to avoid stray/ambient light interference. Also, the housing includes a chip to monitor LED intensity variations. The output is a measure of the refractive index which is generated by the signal processor. The setup also consists of a temperature sensor to remove the effect of temperature variations and to measure accurately the refractive index. The Spreeta setup has been modified and used for bio-sensing applications.⁷²

4 Multiplexed Biosensor Applications

As a consequence of the intrinsic complexity of biochemical pathways (usually changed in disease states),⁷³ it has become established that multiplexed analysis (compared to conventional single-parameter assays) can offer a better biomolecular perspective of the onset of disease and its advance. A high throughput analysis of interactions also helps in understanding factors associated with it in real time. Both of these i.e. multiple analyte detection and high throughput screening drive the multiparameter technology.⁷⁴

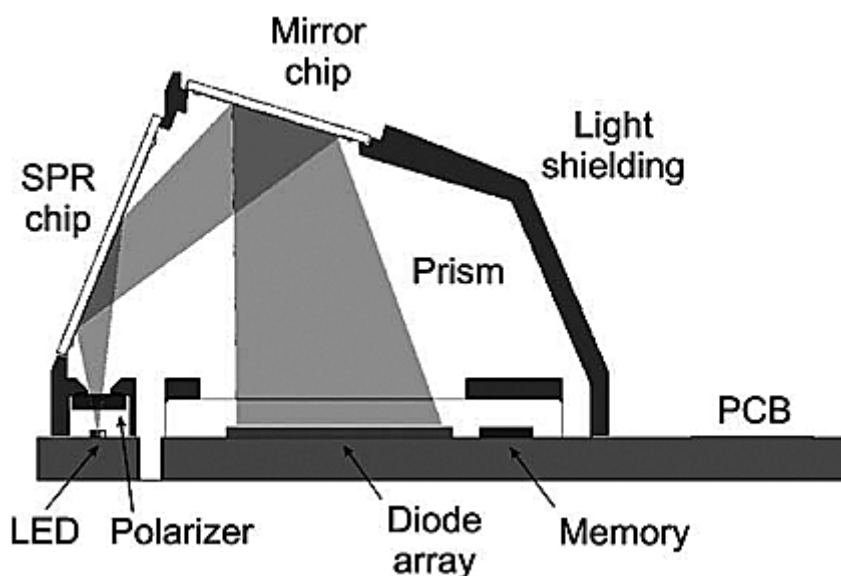


Figure 19: Cross-section of Spreeta 2000, indicating the light path and position of various components.⁷¹

4.1 Multiplexing using different label free optical sensing techniques

As mentioned earlier, one of the most promising technologies for multiplex/multianalyte detection is SPR. This is being performed in various formats in which multiple channels or micro arrays are created on a sensing surface and detection is performed using SPR microscopy or imaging SPR (iSPR). iSPR technology has ushered in microassays for high throughput analysis by the simultaneous screening of the analytes under consideration.

In the early stages of development, a multichannel SPR sensor consisted of a light source capable of exciting surface plasmons in multiple areas of a sensor chip and a detector system capable of detecting reflected light resolved into different co-ordinates of the same detector.⁷⁵ Later developments included detection of reflections on separate detectors;⁷⁶ and wavelength division multiplexing to increase the number of sensing channels by applying different wavelengths at different points.^{77,78}

4.2 SPR Imaging (iSPR)

Homola *et al.*, 2005 developed a multichannel SPR sensor based on wavelength division multiplexing of channels to detect multiple analytes.⁷⁹ Boozer *et al.*, 2006 used this multichannel biosensor and applied their reported proof of concept for multiplexing by simultaneously detecting three fertility hormones: the human chorionic gonadotropin, the human luteinizing hormone, and the follicle stimulating hormone on the principle of SPR.⁸⁰ The iSPR apparatus consists of a p-polarized light source connected with a beam expander and a CCD detector to detect reflected light from the surface under consideration. The image is corrected from the background noise and is analyzed to extract binding curves as seen in Figure 20.

Huang and Chen, 2006 applied the technique of SPR imaging to protein arrays. They detected the presence of 4 proteins: bovine serum albumin (BSA), poly-L-lysine (PL), casein and lactate dehydrogenase (LDG) and also saw the change in the SPR signal during the denaturation of proteins.⁸¹

Dong *et al.*, 2008 demonstrated the application of the SPR imaging technique for multiplexed analysis of Human immunoglobulin G-antibody interactions and they achieved an LOD of 6.7 nM IgG.⁸²

4.3 SPR

Piliarik *et al.*, 2005⁸³ demonstrated an SPR sensor generating a high contrast SPR image by merging iSPR with a polarization contrast and a multilayer SPR structure. They fabricated a chip with 216 sensing spots or 216 surface plasmon active areas with two types of multilayer structures, which exhibited diametrically opposite effects to the change in the refractive index of the sample. These spots were paired up forming a total of 108 channels. Light reflected from the uncoated areas of the chip surface was removed using a polarizer. This led to a high contrast SPR image and minimized cross talk between sensing spots. The sensitivity was increased and immunity towards input light intensity fluctuations was achieved by taking the ratio of the intensities of light reflected from the two different types of spots in a pair. The Refractive index resolution was measured as 3×10^{-6} refractive index unit (RIU). Initially, this novel design suffered from low reproducibility and reduced sensitivity which was addressed by using the microspotting method for immobilizing oligonucleotide probes which created 80% more binding sites and gave an LOD of 100 pM. The sensitivity was further improved (refractive index resolution $\sim 2-3.5 \times 10^{-7}$) in 2008 by adding a self-referencing feature to the sensor system. In this design, two mirrors, formed at the bottom of the prism were used to provide a dynamic reference for the dark current correction of the detector and to provide dynamic referencing for fluctuations in the intensity of incident light (Figure 21).

On adding microspotting to this sensor, Piliarik *et al.*, in 2009, could achieve a refractive index resolution of 2×10^{-7} RIU and a pathogen LOD of 100 pM.⁸⁵ Later in 2010, they went on to demonstrate high-throughput screening of protein biomarkers in diluted blood plasma. A high density protein array of 120 sensing spots was made by the microspotting method by immobilizing antibodies

Multianalyte detection:
Detection of more than one analyte simultaneously.

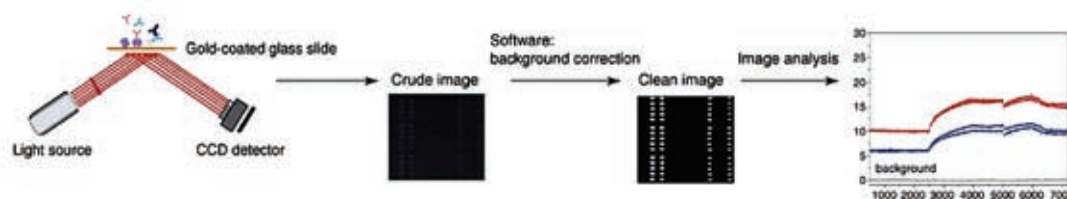


Figure 20: A schematic representation of SPR imaging.⁸⁰

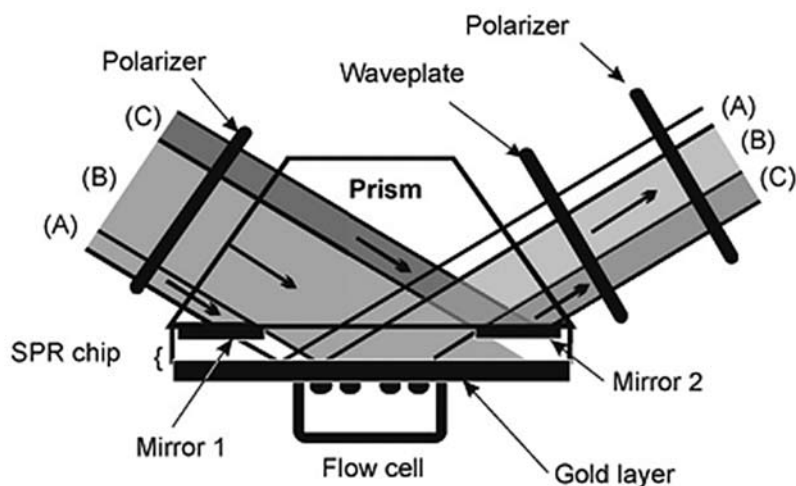


Figure 21: SPR imaging with self-referencing and polarization contrast. Mirror 1 blocks part (A) of incident light and thus the detectors corresponding to that part of the sensor surface provide a reference for the dark current of the detectors since no light is reflected on to the detectors. Mirror 2 reflects part (C) of incident light to the detector for referencing against light source fluctuations.⁸⁴

on the sensing spots and the remaining area was blocked by covalently immobilizing BSA to avoid non-specific adsorption on the surface. Using gaskets made up of adhesive material, they divided the SPR chip into 5 channels in an acrylic flow cell. Each channel had two pairs of 12 sensing spots, one spot for reading and a second spot for reference. They detected multiple cancer biomarkers like human chorionic gonadotropin (hCG) and an activated leukocyte cell adhesion molecule (ALCAM) with an LOD as low as 45 ng/mL for ALCAM and 100 ng/mL for hCG in blood samples.⁸⁶

One of the major issues that any biosensor faces is the fact that the target molecules may not come close enough to the sensing surface to be captured. In this regard, Krishnamoorthy *et al.*, 2009⁸⁷ demonstrated the use of electro-osmotic flow (EOF) for sample transport and electrokinetic focusing (EKF) for guiding the samples to specific array locations in iSPR. The channels were fabricated of PDMS by using replica molding⁸⁸ which was attached to the supporting substrate by a stamp and stick bonding technique.⁸⁹ The gold array was patterned on a glass chip by electron beam evaporation. The device was further improved⁹⁰ by forming 12 channels with 12 gold islands each (Figure 22). Limitations in iSPR camera dimensions allowed measurement of only 9 analytes (Anti-BSA, Anti-HSA, Anti-HIgG, Anti-neomycin, Anti-gentamycin, Fab specific AHIgG, F(ab)₂ specific AHIgG, Fc specific AHIgG and Anti-β2M) along with a reference channel. The system had the ability to check reproducibility without repeating experiments as

each channel measured the sample at 12 spots. The device suffered from problems of steric hindrance, due to the presence of capture ligands that were larger than the analyte molecules and target molecules sticking to the surface of PDMS.

Multiple analyte detection has also been achieved by Wavelength Division Multiplexing (WDM) of channels.⁹¹ A special ATR prism coupler has been used which produces two SPR dips at region A and Region B as shown in Figure 23. Refractive Index resolutions of 1.3×10^{-6} RIU were observed in region A and 7×10^{-7} RIU in region B.

SPR-based sensors for multiple analytes have also been developed using diffraction gratings using a configuration termed a surface plasmon resonance coupler and disperser (SPRCD).⁹²⁻⁹⁴ In SPRCD, as light is incident on a gold coated diffraction grating, a portion of the light in second order diffraction excites the surface plasmon wave and light diffracted in the first order forms the wavelength spectrum. The light is finally reflected off a toroidal mirror onto a CMOS detector array (Figure 24). This eliminates the need of an external spectrophotometer.

Diffraction gratings were fabricated using the holographic method.⁹⁵ A master grating was developed using the interference pattern of laser sources in an optical setup. The generated sinusoidal pattern on photoresist acts as a master for soft lithography-based grating fabrication.⁹⁶ Polydimethylsiloxane (PDMS) poured on the master grating was heat cured and then peeled off from the master grating as shown in Figure 25. This PDMS

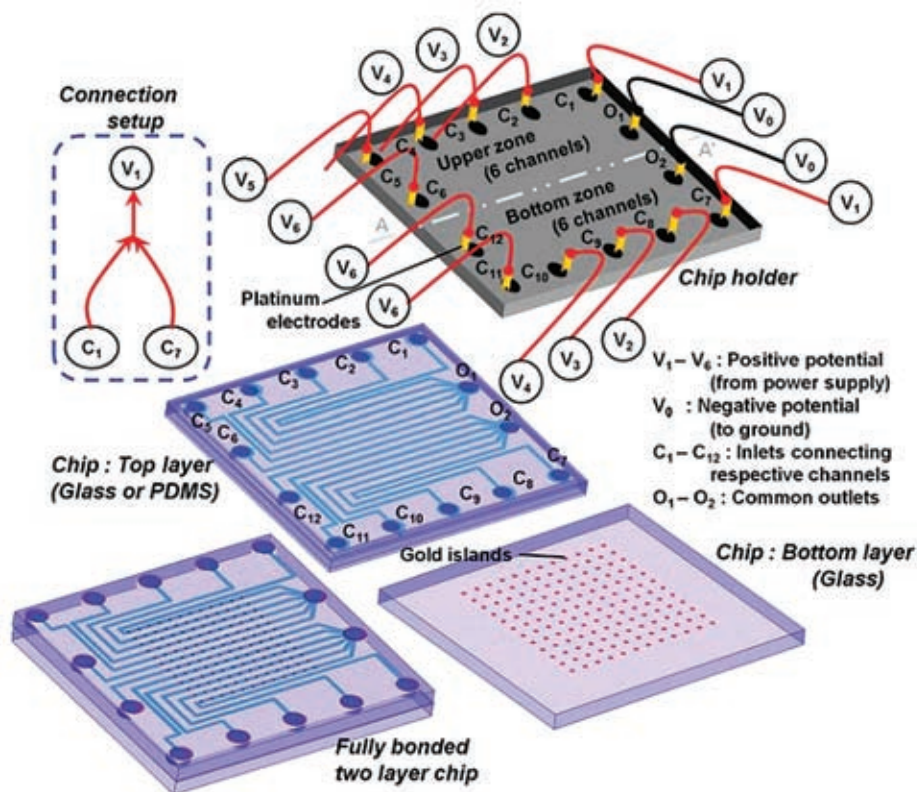


Figure 22: Illustration of a PDMS/Glass chip having 12 channels on a PDMS surface and 12 gold islands on glass, platinum electrodes were connected to the supply.⁹⁰

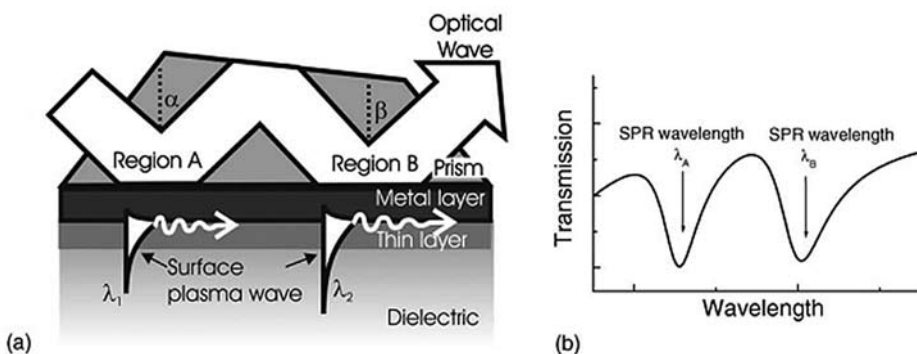


Figure 23: (a) Concept of WDM using a special prism and (b) Two SPR dips at region A and B.⁹¹

structure acted as the elastomer stamp. This stamp was then placed on top of a UV-curable polymer which was spun on the substrate. The polymer was exposed and then the stamp was removed. A film of gold was deposited on the replica obtained from the PDMS stamp.⁹⁷ This formed the grating used in the SPRCD structure. The SPRCD cartridge was made by clamping a 6 channel gasket to an SPRCD chip (Figure 26). The LOD observed were $0.30 \mu\text{gL}^{-1}$ for enrofloxacin (ERFX), $0.29 \mu\text{gL}^{-1}$

for sulfapyridine (SPY) and $0.26 \mu\text{gL}^{-1}$ for chloramphenicol (CAP).

Akwoah *et al.*, 2010 did a theoretical study on dual channel planar waveguide SPR.⁹⁸ The channels had gold and silver SPR active areas, and showed distinct SPR dips when immersed in liquids of different refractive indices. Multianalyte sensing has also been achieved using ingeniously designed flow systems. Springer *et al.*, 2010 demonstrated a multichannel (4 channel) SPR sensor

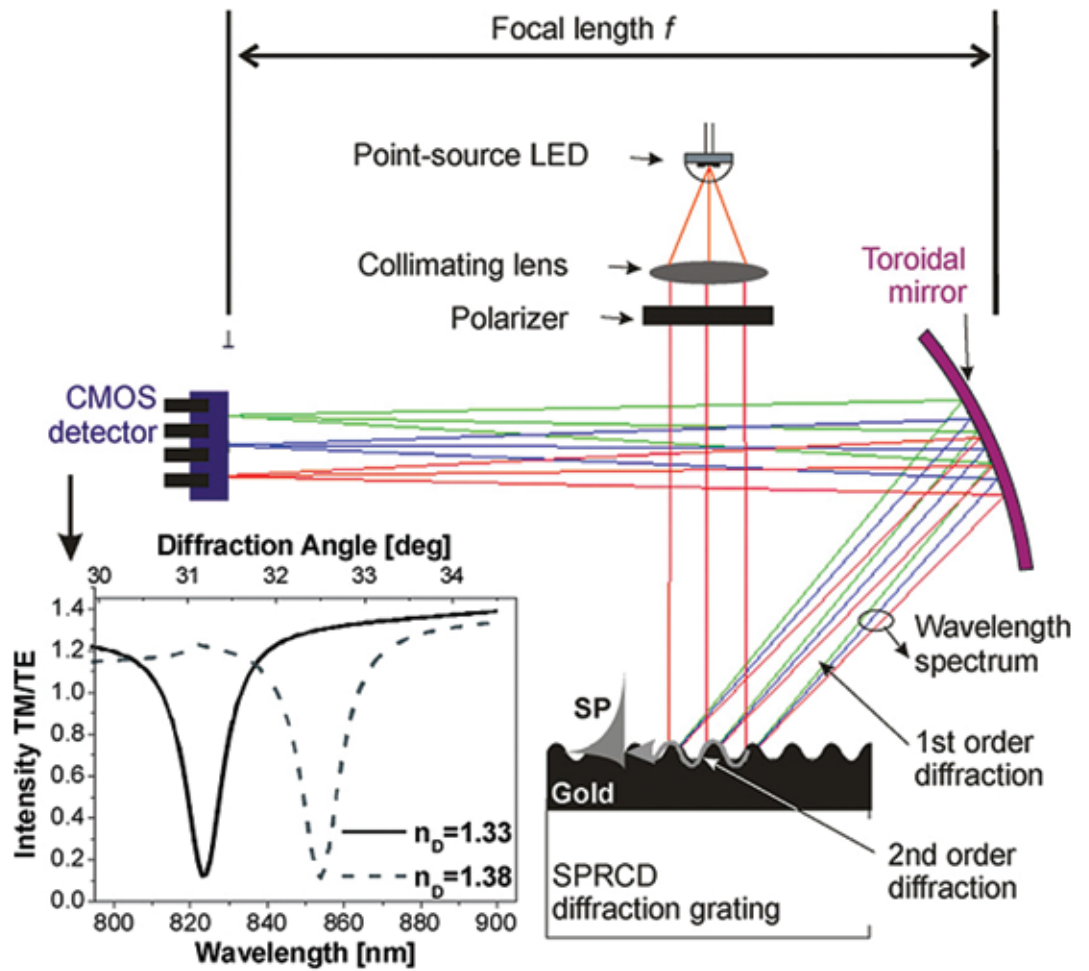


Figure 24: Concept of SPRCD.⁹⁴

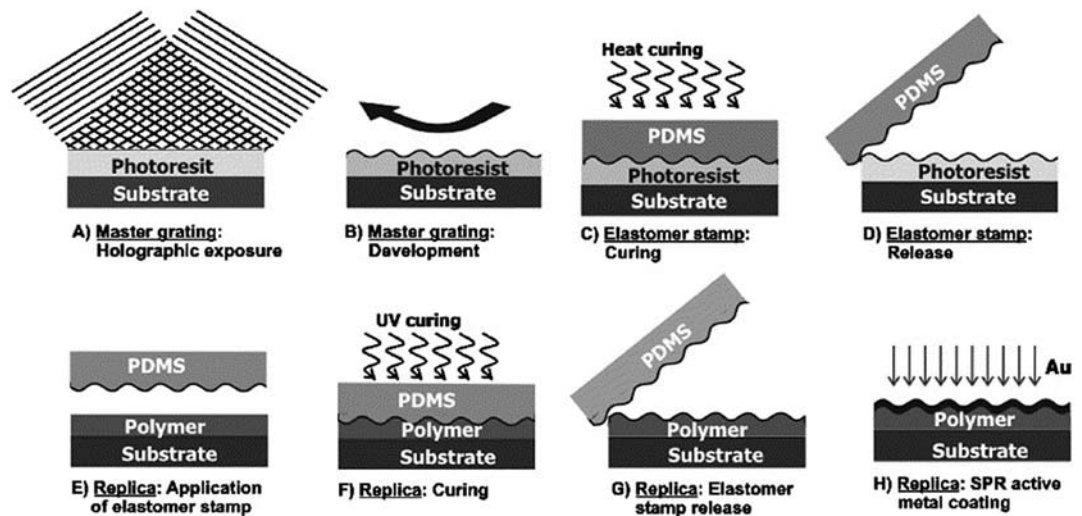


Figure 25: Fabrication steps of diffraction grating.⁹⁷

detecting nucleic acids with an LOD of 3 fM in 4 min. As shown in Figure 27 the flow system has two states and in each state a different sample is allowed to flow over the sensing region.⁹⁹

Olkhov and Shaw, 2010 used microarray imaging to detect 4 proteins and to analyse

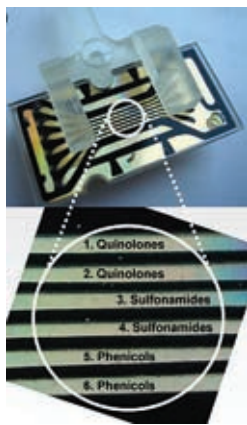


Figure 26: Image of an SPRCD cartridge for detection of antibiotics.⁹²

antigen-antibody interaction. They used an inkjet printer to print an array of gold nanoparticle seeds on the surface. Thereafter, the seeds were grown to the required size and functionalized with the aid of an inkjet printer.¹⁰⁰ The LOD achieved was 250 ng/ml.¹⁰¹ The capability of multiplexed SPR sensing for multianalyte detection was significantly extended when Ouellet *et al.*, 2010 came up with a microarray design using iSPR technology.¹⁰² Utilizing microfluidics enhanced fabrication, a sensing platform was formed that could detect 264 analytes at a time. A PDMS layer was fabricated using soft lithography.¹⁰³ Up to 6 different concentrations of an analyte could be made on a chip, by a series of micromixers which diluted the analyte concentrations. Micro-pumps aided delivering the analytes to specific chambers and digital control helped in selecting particular chambers to be monitored. The details of the design are shown in Figure 28. There are six columns of 11 groups, each having four chambers. Row multiplexers were used to select a group of 4 chamber based binary control inputs. Samples

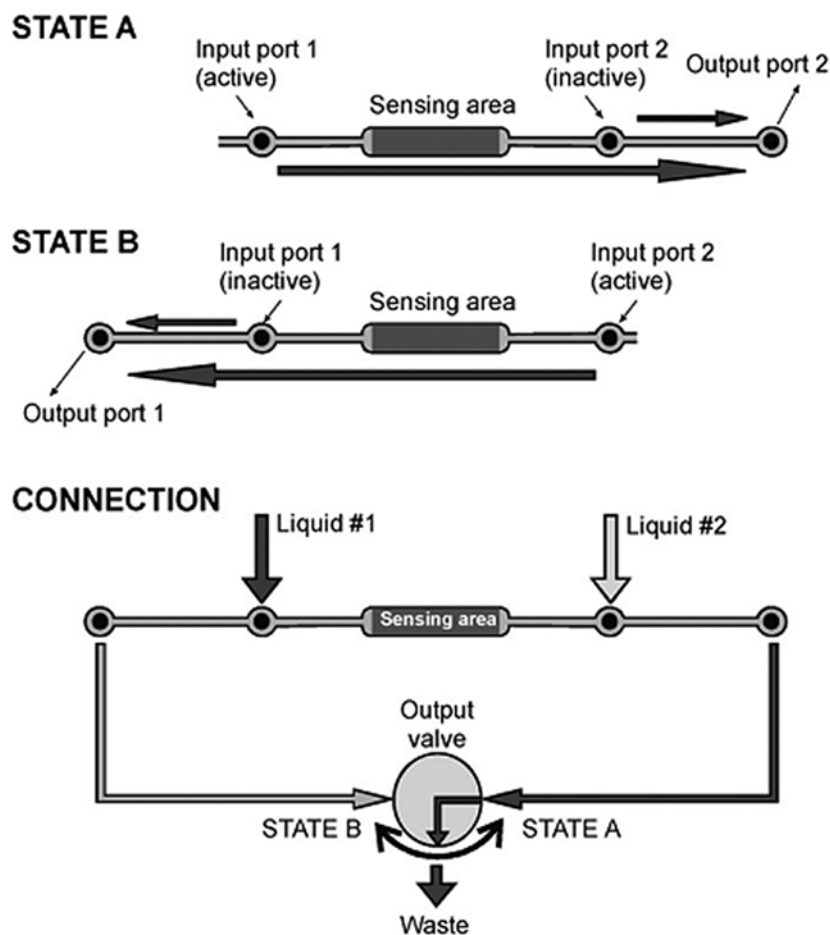


Figure 27: Schematic shows connections of sensing area to ports in different working states.⁹⁹

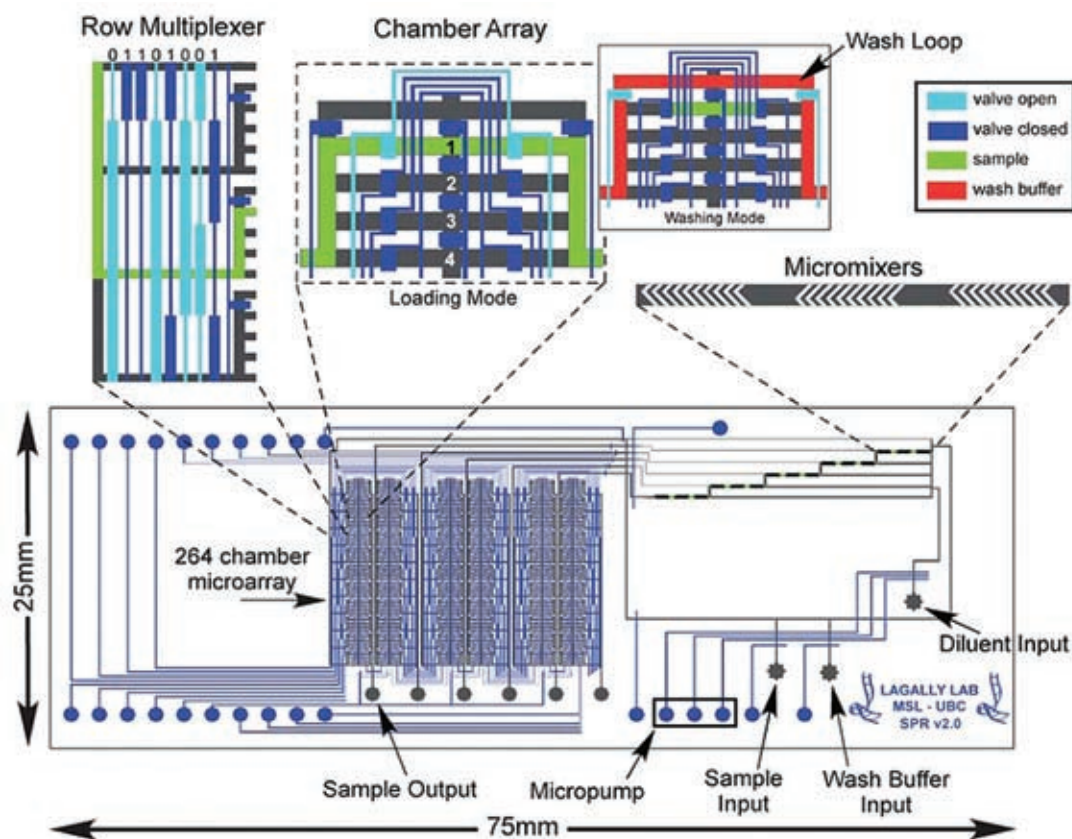


Figure 28: Schematic of microfluidic array.¹⁰²

were loaded on to particular groups using an arrangement of valves which directed the sample appropriately (for example, in the Figure 28, green indicates that the valve of chamber 1 is open). Each sample loading was followed by a wash loop that removed remnant samples in the microfluidic path.¹⁰²

In the area of multichannel SPR detection, a modified Polymerase Chain Reaction (PCR)-SPR setup was used to simultaneously detect pathogens (*Pseudomonas aeruginosa*, *Staphylococcus aureus*, *Clostridium tetani* and *Clostridium perfringens*) using a single stranded DNA (ssDNA) amplification scheme.¹⁰⁴ The complete scheme is shown in Figure 29. Pathogen specific complementary DNA probes were immobilized in line at a sufficient distance from each other on the gold film. The SPR setup was used in the Kretschmann configuration. The DNA of the bacteria was extracted and added to PCR for amplification. These PCR output was used as the input sample for SPR. The sample was recirculated in order to increase sensitivity.¹⁰⁵

To increase resolution in multichannel sensing, a spectral/wavelength interrogation technique has also been explored. Depending on the capabilities of the recording spectrophotometer,

spectral interrogation can have better resolution. However, for sensing multiple channels/spots, a corresponding number of spectrophotometers and collimator pairs are required.^{91,106} One of the possible cost-effective alternative methods is to use a programmable aperture for a spectrophotometer, described in a technique called spatial light modulation (SLM). The step by step process to collect output using SLM is shown in Figure 30. SLM has two states for its pixels: open i.e. transparent and closed i.e. opaque. Initially SLM pixels are set open. The active area of SLM is limited to the area of the aperture. Then regions of interest are identified and assigned to numbered channels. To remove background noise, SLM is closed and the background signal reference is recorded. Then one at a time, all the Region of Interest (ROI) areas are opened and signals are collected. The background signal is subtracted from the signals and high resolution SPR spectra are obtained. Sutapun *et al.*, 2008 demonstrated a prototype 5-channel setup made of PDMS by using the aluminum molding technique.¹⁰⁷ As may be obvious, the ability to measure the kinetics of reactions is limited by the rate at which all the ROIs can be cycled through. This technique, while introducing

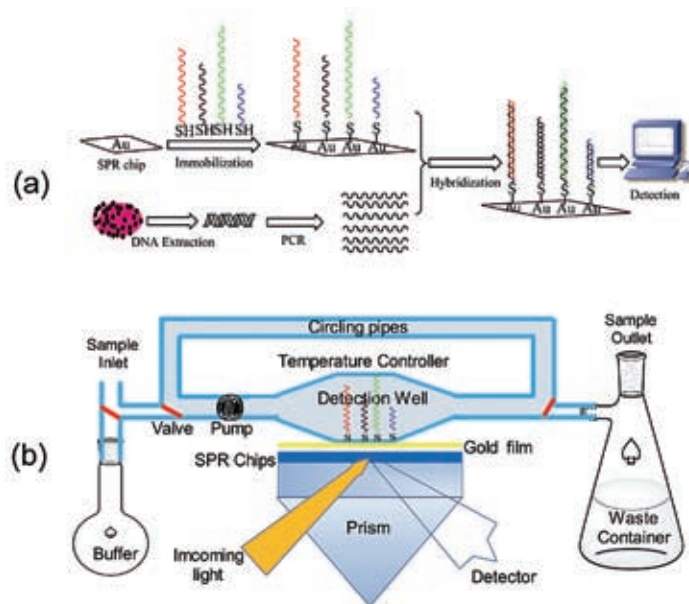


Figure 29: (a) Complete step from immobilization to hybridization and detection; (b) Modified SPR setup.¹⁰⁴

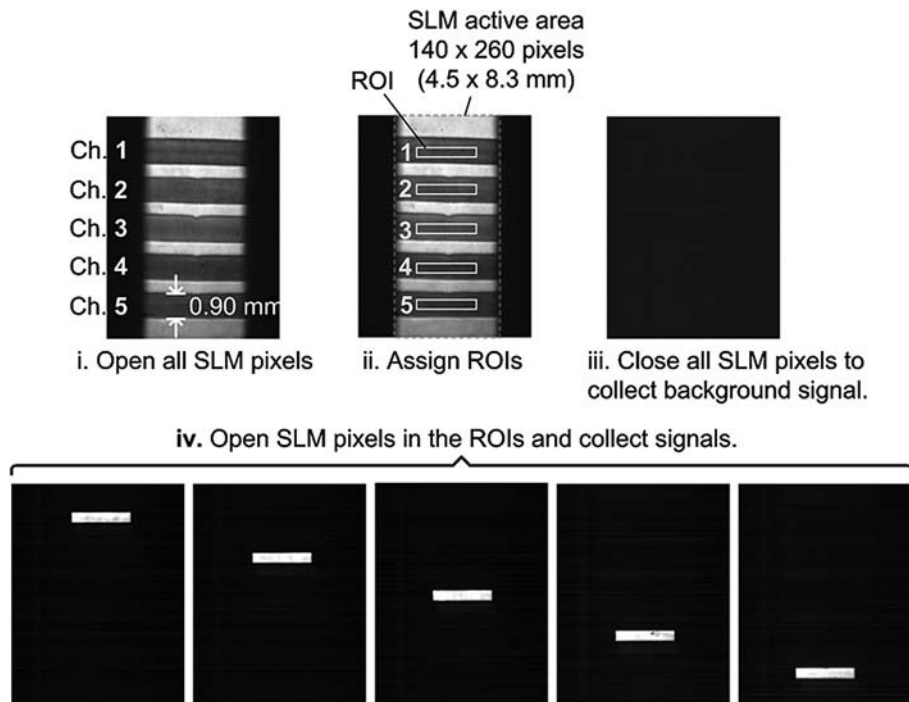


Figure 30: Operating procedures for collecting signal using SLM techniques.¹⁰⁷

the possibility of using spectral interrogation in conjunction with a multichannel SPR setup, also provides the flexibility of obtaining data from array spots of any size and at any position on the substrate¹⁰⁸ limited only by the SLM spatial resolution. Therefore, many different methods

like micro spotting, inkjet printing, *etc.* can be explored for creating arrays.

The coupling of light using SPR substrates has also been achieved using diffraction gratings. Thirstrup *et al.*, in 2004 presented a novel design using polymeric diffractive optical coupling

elements (DOCE) in conjunction with SPR sensors for multiplexing and ease of miniaturization. An injection-molded COC polymer chip integrated with two DOCEs replaced traditional prism and focusing optics for coupling light in and out of the SPR substrates (Figure 31(a)). The input light was collimated and projected perpendicular to the input DOCE surface. Because of mirror symmetry of the DOCE elements, the input light is focused to a point at the centre of the sensor element at different angles as can be seen in Figure 31(b). At the output side reflected light is converted to a parallel beam incident on different positions of the detector array. The gratings were fabricated using a holographic writing technique¹⁰⁹ involving two different lasers at two

different angles to expose a photoresist to get the desired structure of the grating. A metal master is made by sputtering and galvanizing nickel on the photoresist. This metal master is used to make the polymer chip by injection molding and finally a gold layer is sputtered on the chip for sensing. The obvious advantage of this scheme lies in its possible parallelization.¹¹⁰ In a parallel effort towards integrating diffractive optics to couple light in an SPR system, Chien *et al.*, in 2009 designed an angular interrogation scheme based multichannel SPR chip using a focusing diffractive optical element (FDOE).⁶⁶

In an extension to phase measurement schemes in SPR configurations,^{111,112} Halpern *et al.*, 2011 demonstrated phase measurements in a micro-

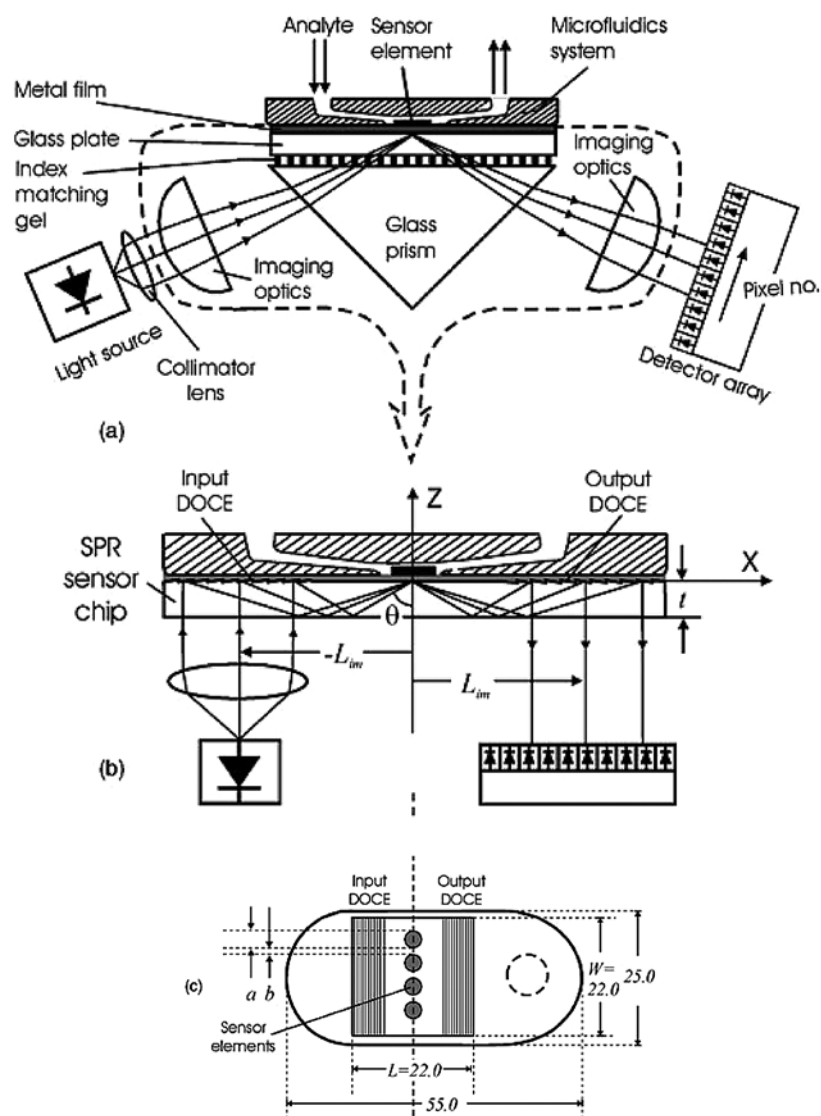


Figure 31: (a) Kretschmann configuration; (b) Modified SPR setup using DOCE; (c) Top view of the polymer chip along with dimensions in mm.¹¹⁰

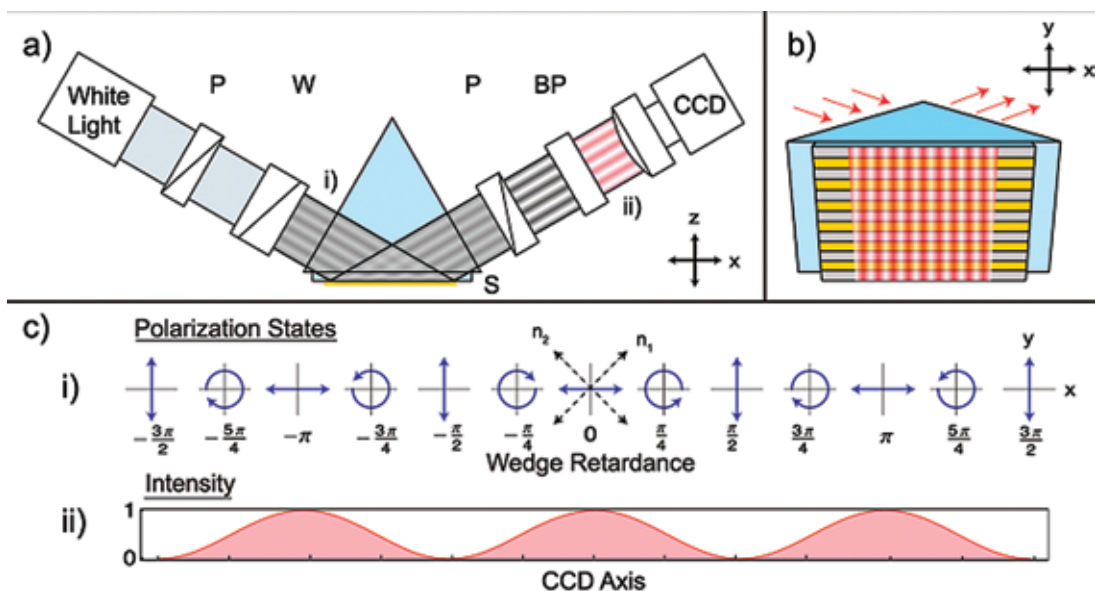


Figure 32: (a) Schematic of SPR-PI showing all the components; (b) Interference Pattern on the sensor surface; (c) Polarization states and Intensity plot.¹¹³

array format by using an SPR- Phase Imaging (SPR-PI) technique (Figure 32), that has the potential to increase the throughput of such measurements. The input light from the source is polarized and is passed through a wedge depolarizer. This creates a spatially distributed periodic polarization pattern on the sensing surface as seen in Figure 32(b). The reflected light passes through an output polarizer which creates intensity fringes related to a phase shift which, in turn, passes through a narrow band pass filter which generates a contrast. Finally, the pattern is detected by CCD.¹¹³

Biacore® was the first to commercialize an SPR apparatus in 1990 and since then many other SPR devices, based on various configurations and formats, have come in to the market. Since this is a very powerful technique that has captured the imagination of many researchers involved in proteomics research, various research groups have published results on the basis of data recorded from one machine or the other.¹¹⁴ One example of this is the ProteON XPR36, which has been used by various researchers for multiplexed analysis. Situ *et al.*, 2010 designed a system with 4 x 4 arrays for label free detection using the SPR technique to detect 16 analytes simultaneously.¹¹⁵ Abdiche *et al.*, 2011 expanded this instrument for 36 ligands and claimed it to be better than Biacore 2000 in terms of the time required for the same application.¹¹⁶ Nahshol *et al.*, 2008 demonstrated the use of ProteON XPR36 to analyze parallel binding kinematics using multiple microfluidic channels.¹¹⁷

4.4 LSPR

As discussed earlier metallic nanostructures have been used for LSPR based sensing for a long time. With the development of various techniques, compatible with standard microfabrication tools, to create such nanostructures on a chip, this area of research has gained significant momentum. It is quite evident that multiplexed sensing systems can be developed using microfabrication coupled with nanostructure formation. Since the characteristics of the LSPR response depend on the size, shape and composition of the nanostructures, various methods have been adopted to create such structures on a chip.

Prabhakar and Mukherji¹¹⁸ demonstrated a C-shaped waveguide coated with gold nanoparticles (GNP) using the single step lithographic processing used by them earlier.⁵⁶ The LSPR sensor had a sensitivity to RI changes better than the bare waveguide evanescent wave absorption sensor developed by them earlier.³⁹ The schematic of the waveguide used in the optical setup is shown in Figure 33. Light enters the waveguide through an optical fiber and propagates by TIR in the bend region. The evanescent wave generated at the interface of the waveguide interacts with immobilized GNP. The energy of the evanescent wave produces oscillations in the metal nanoparticles leading to localized surface plasmons. The sample under study flows through the microchannel which interfaces the bend region causing a change in the RI of the medium and thereby a change in the evanescent absorption characteristic.

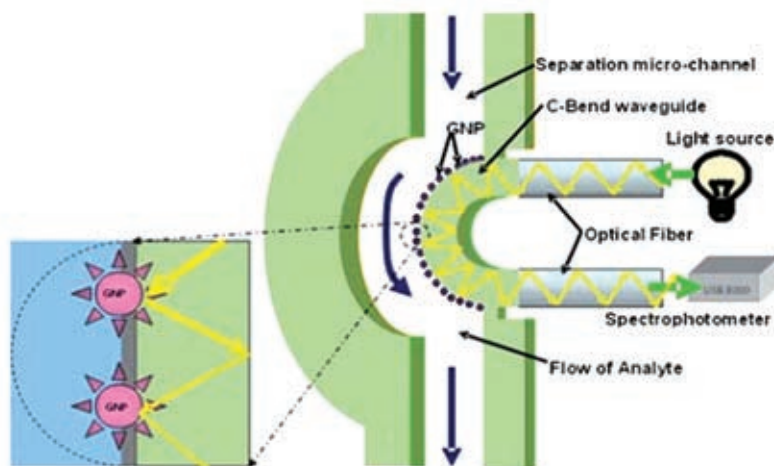


Figure 33: C-bend waveguide coated with GNP for LSPR based detection. The closet on the left shows the generation of surface plasmons due to the interaction of an evanescent wave and GNP.¹¹⁸

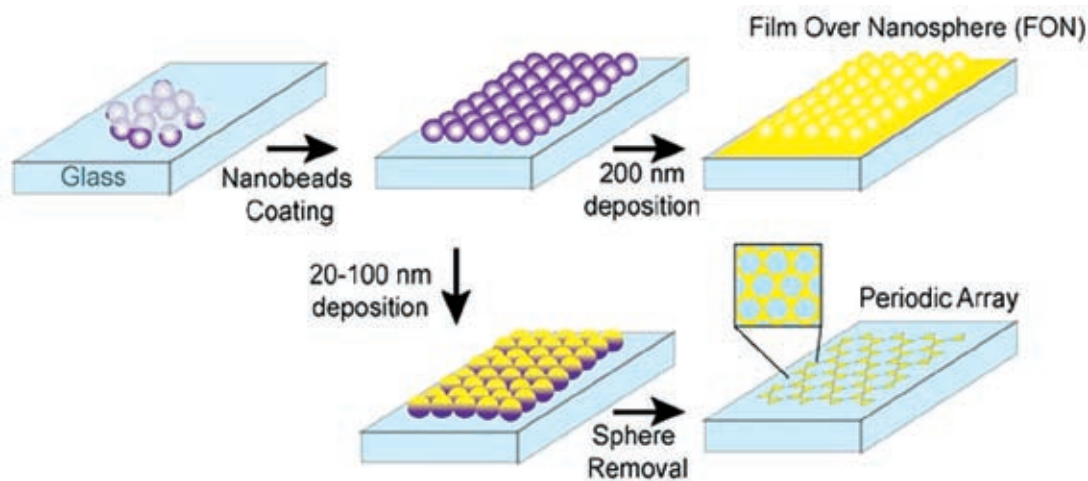


Figure 34: Steps in Nanosphere Lithography (NSL) to fabricate periodic nanoarrays.¹²¹

As size, arrangement, shape and material properties like the dielectric of nanoparticles are important in determining LSPR wavelength, a controlled synthesis of nanoparticles and a controlled arrangement of nanoparticles in the sensing region is important for the efficient use of LSPR. Many synthesis and fabrication methods for nanoparticles, nanostructures and nanoarrays are now available. We will look at some of the methods used for the fabrication of nanoparticle arrays.

Nanosphere Lithography (NSL) is one of the most common methods for nanoarray fabrication. The process involves an assembly of nanospheres made of polymers or some other material which can be dissolved or lifted off from the surface easily after being subjected to deposition of a metal by sputtering or vapor deposition methods. A schematic showing the steps for NSL is shown in

Figure 34. The substrate is cleaned and chemically modified (if required), so that the spheres can freely move and assemble on the surface. The spheres, along with a suitable dispersing medium, are drop-coated on the substrate. As the dispersing medium slowly evaporates, the nanospheres come closer and form a hexagonal close pack (HCP) structure on the substrate surface. This HCP is commonly termed a nanosphere mask. Once the self assembly of the nanospheres is complete, a metal layer of desired thickness is deposited on top of the microsphere mask. This layer is commonly termed metal film on nanosphere (FON). This plasmonic layer can be used as a stable substrate in various applications like SERS.¹¹⁹ For fabricating LSPR devices, the substrate is then sonicated in a solvent to dissolve away the nanospheres and along with them remove the metal

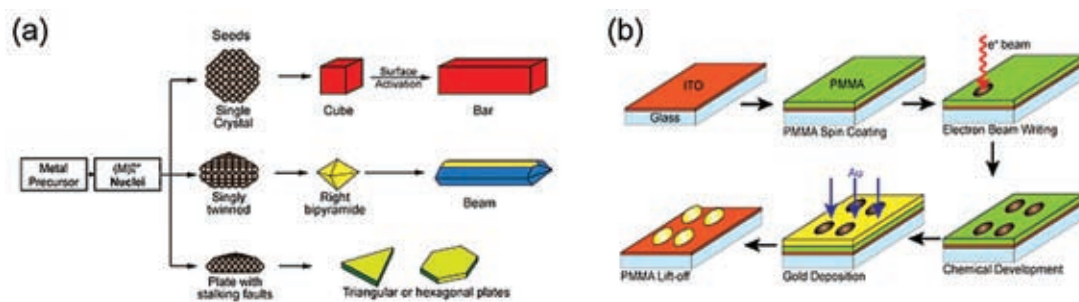


Figure 35: Techniques for fabrication of nano structures; (a) Chemical synthesis; (b) General steps for EBL.¹²¹

deposited on the surface of the spheres, leaving an array of triangular nanostructures on the surface of the substrate.¹²⁰

To fabricate nanowells, the process is slightly different. Instead of depositing metal on the HCP, the substrate and the assembled HCP on it is processed in a reactive ion etcher (RIE) to get the desired nanowell depth (Obviously the nanospheres in this case have to be resistant to reactive ion etching). This creates an array of pits in the areas between the spheres. Then, instead of depositing metal film, the structure is sonicated to remove the nanosphere giving an array of pits and a metal layer is deposited to get a metal surface with an array of nanowells.¹²² For getting the desired shape and structure using NSL, modifications can be performed at various steps of the process. NSL is rapid and cheap for fabricating many structures at the same time. However, since it is critically dependent on the shape and self-assembly properties of the nanospheres, it may have some defects like vacancies at some spots, polydispersity, line defects (slip dislocations), *etc.*¹²³

Electron-beam Lithography is another popular technique for fabricating arrays of nanostructures on substrates. The main advantage of this technique over NSL is that it can fabricate nanoparticles of any shape and size with high accuracy. An electron sensitive resist is spin-coated on top of the substrate. The structure to be patterned is programmed into the system, and based on that, an electron beam scans over the surface to “write” the desired pattern and expose the resist. The remaining structure is removed and a metal layer is deposited. This has been used to fabricate nanoparticles of different shapes and sizes.¹²³ The fabrication steps are shown in Figure 35(b).

There are many other fabrication techniques like focused ion beam (FIB) milling,¹²⁴ dip-pen lithography,¹²⁵ *etc.* which provide control over the size and shape of the structures. Chemical synthesis methods (Figure 35a) have also been used for making nanoparticles on a substrate but they may

also exhibit polydispersity of nanoparticle size which has to be taken into account and reduced by optimizing the process.

Many conventional and novel fabrication techniques for nanopatterning are explained in a review by Stewart *et al.*, 2008 which was followed by another review explaining nanofabrication techniques based on soft-lithography, along with an analysis of the effect of different dimensions on the spectra obtained.¹²⁶ All the techniques provide flexibility to modulate the shape, size and distribution of nanostructures, thereby selecting a working range of LSPR from the visible to the infrared region.^{127,128}

Zhu and Zhou, 2011 fabricated an array of pentagram or star-like structures for application in an LSPR-based nanobiosensor.¹²⁹ They did the theoretical modeling of the device to design its structure and also to find out field distribution over its surface. Their calculation indicates it has high potential for applicability as a substrate for an LSPR based biosensor. Nanofabrication was done using the FIB technique by sputtering silver over the substrate milling out pentagram arrays.

Another excellent LSPR array of nano-cones were designed by Wu *et al.*, 2010¹³⁰ using nanoimprint lithography (Figure 36). The silicon master was made using the Bosch RIE process.¹³¹ Different etchants with different *etch* rates for Silicon were used with deep RIE to create silicon cones on the wafer. Using UV-Nano Imprint Lithography an array of conical nanoholes was created on a polymer substrate. This nanohole array was used to create an array of nanocones on a different polymer substrate and a layer of gold was deposited to create gold-coated polymer cones.

The main aim of the iSPR technique was to take SPR sensing to high throughput parallelized sensing. As we saw, iSPR has been used in the Kretschmann configuration. One of the major limitations of this configuration is the use of a prism in the setup since it reduces the field of view, limits the scope of miniaturization and

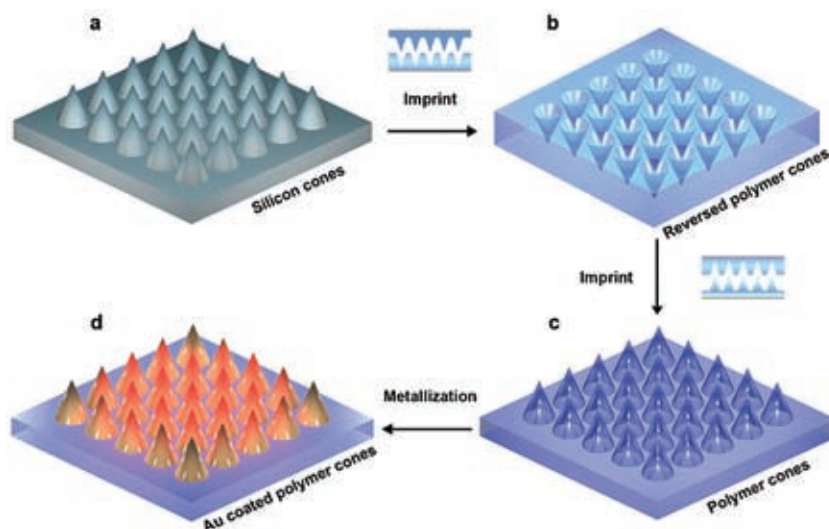


Figure 36: Steps for fabricating 3D cones using nanoimprint lithography; (a) Silicon master; (b) Reverse polymer cones made after imprinting into the polymer layer; (c) Polymer cones made from reversed polymer cones; (d) Gold deposited on top of the cones.¹³⁰

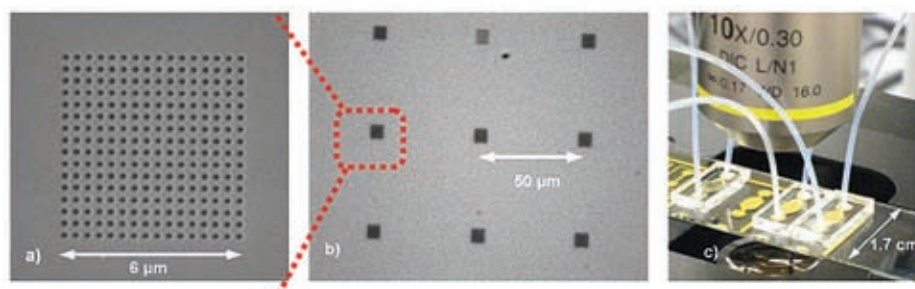


Figure 37: (a) Scanning electron microscopy (SEM) image of a 16 × 16 nanoarray; (b) Bright-field microscope image of a part of 5 × 3 microarray; (c) Microfluidic flow cell along with tubing.¹³²

requires optics with low numerical apertures.¹³² Research by Ebbeson *et al.*, 1998¹³³ and Martin-Moreno *et al.*, 2001¹³⁴ about enhanced optical transmission (EOT) in a periodic array of metal nanohole structures led to the use of nanohole arrays with SPR. They reported that surface plasmons on the top and bottom of the gold film are coupled through nanoholes at specific wavelengths. The wavelength is dependent on the refractive index of the sample and its surroundings, and also on the dimension and periodicity of the array. Basically, the nanoarrays act as couplers which convert light to surface plasmons on one side and surface plasmons to light on the opposite side. This property makes nanohole arrays good substrates for SPR sensing without the need of a prism by transforming the setup to utilize simple collinear optics. This was applied to biosensing by testing it in a transmission mode for monitoring biomolecule adsorption. 11-mercaptoundecanoic acid

(MUA), along with Bovine serum albumin (BSA) adsorption was successfully detected by Brolo *et al.*, 2004.¹³⁵

Stark *et al.*, 2005 designed a nanohole array and sensing was based on monitoring changes in the intensity of EOT. They demonstrated high refractive index resolution (9.4×10^{-8} RIU) in the setup, which is better than conventional SPR and EOT sensing using wavelength interrogation.¹³⁷ Ji *et al.*, 2008 further developed 25 nanoarrays for multiplexed detection based on intensity sensing. On this nanoarray, 25 separate binding curves between glutathione S-transferase (GST) and anti-GST were measured in real time to demonstrate multiplexing.¹³⁷ This method was found to be suitable for multiple analyte measurements than the previously reported method by De Leebeek *et al.*¹³⁶

Lesuffleur *et al.*, (2008) demonstrated the potential of nanohole arrays based on the phenomena of EOT for high throughput scanning

SPR imaging.¹³² They used a He-Ne laser source to improve detection sensitivity. They fabricated a 16×16 nanoarray using a focused ion beam technique on a gold-chrome coated glass substrate. Each nanohole had a diameter of 200 nm with a periodicity of 380 nm to 460 nm. A 5×3 microarray of such nanoarrays, each spaced at a distance of 50 μm from each other, was fabricated (Figure 37). A flow cell was fabricated using the soft lithography technique. A master mold was made using SU-8 and the pattern of 100 μm deep channels was transferred to PDMS. The detection setup had a He-Ne laser illuminating from the bottom of the chip. The optics was simplified due to the absence of a prism and the generation of surface plasmon waves directly from the nanoarrays. The transmitted light was detected using a 10x objective lens and imaged using a CCD in line on the opposite side of the chip. They optimized the array periodicity by measuring the kinetics of self-assembling monolayers at different periodicities. Im *et al.*, (2009) demonstrated the applicability of the same setup for parallel measurements of molecular binding kinetics, by integrating a six-channel microfluidic chip to the SPR setup. The nanohole size was reduced to 150 nm from 200 nm to accommodate more nanoholes on a single chip.¹³⁸

Yang *et al.*, (2009) demonstrated multiplexed analysis using nanohole arrays which acted as a nanoplasmonic probing platform that exploited EOT.¹³⁹ They had already used the platform to detect single molecules (anti GST, LOD: 10 nM) and analysis of biorecognition events.¹⁴⁰ They showed multiplexing by fabricating 20 nanoarrays having different dimensions and periodicity, which consequently led to different nanostructures having different optical behaviors. They demonstrated analyte detection by passing NaCl, Coomassie blue, bovine serum albumin, and liposome solutions over the nanostructure surface. However the system developed had low refractive index resolution, in the range of 10^{-4} RIU, which is less than the conventional SPR.

Endo *et al.*, (2006) developed a multiarray optical nanochip based on the principle of localized surface plasmon for high throughput screening. The multi array provided 300 nanospots with a core shell nanoparticle layer. In this case the LSPR nano chip was constructed by evaporating gold on a glass substrate and allowing a SAM of silica nanoparticles on the gold surface by modifying the surface chemistry. On top of the silica nanoparticle monolayer, gold was again evaporated. Thus, the silica nanoparticles act as a core and the top and bottom gold layers act as a shell (Figure 38). Light

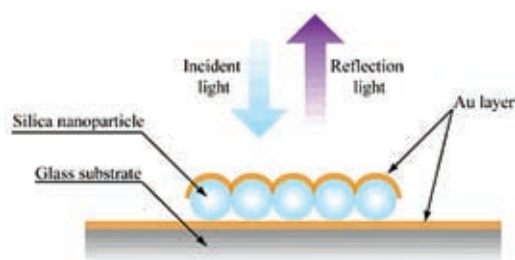


Figure 38: Core shell configuration for LSPR nanochip.¹⁴¹

was incident on the top of the surface through a fiber and reflected light having LSPR spectra was detected back by the fiber. Six different antibodies (Antibodies against IgA, IgD, IgG, IgM, CRP, and fibrinogen) were immobilized at this spot.¹⁴¹ The antigen concentrations were determined by passing each sample through the complete array and it was quantified with respect to the peak absorption intensity of the LSPR spectra obtained. The detection LOD observed was 100 pg/mL.

Piliarik *et al.*, in 2012 have published the design of an LSPR imaging based biosensor using a gold nanorod array.¹⁴² They demonstrated similar sensitivity to LSPR imaging based sensors using a polarization contrast¹¹¹ by demonstrating detection at sub nanomolar concentrations. The Polarization contrast helps in taking advantage of the changes in both amplitude and phase of the reflected light. The polarized light was incident on the prism. The TIR at the prism metal interface causes an evanescent wave which excites the LSPR. When polarized light interacts with the surface, it becomes elliptically polarized on reflection from the surface. The parameters of the ellipse are dependent on the refractive index near the surface. This elliptically polarized light passes through a waveplate which causes a phase shift in TM and TE components. The output polarizer again linearly polarizes the reflected light. The enhanced output goes to CCD (Figure 39). A nanorod array was fabricated using e-beam lithography. They demonstrated the application of this array for oligonucleotide detection by detecting on an average one DNA per nanoparticle.

4.5 RIfS (Reflectometric Interference Spectroscopy) and SRIB (Spectral Reflectance Imaging Biosensor)

RIfS has found its application in High throughput scanning⁴² and for performing binding studies.¹⁴³ Birkert and Gauglitz (2002) demonstrated RIfS for the development of a parallel affinity assay for thrombin inhibitors. Plastic microplates with 96 wells and 384 wells were used for sensing and were

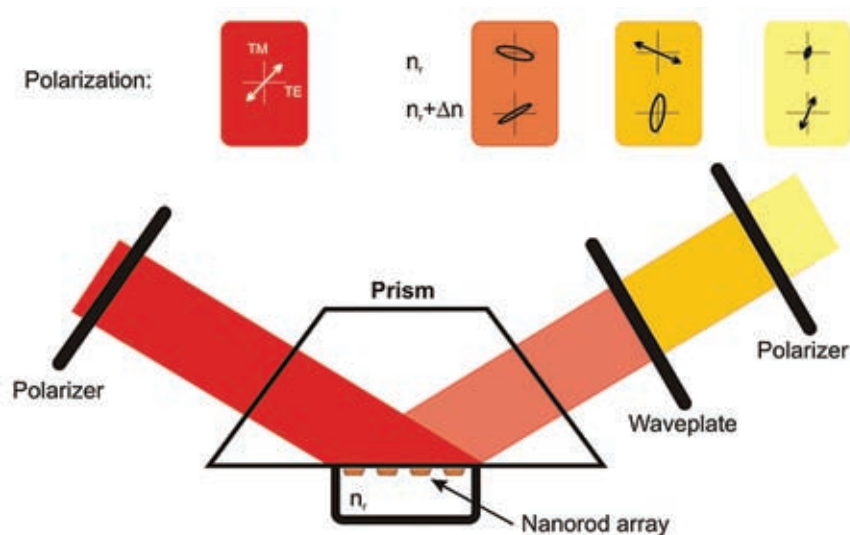


Figure 39: Schematic of an LSPR based optical biosensor using nanorod arrays along with polarization at different positions.¹⁴²

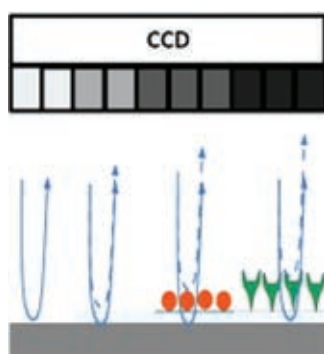


Figure 40: Principle of SRIB: Relative reflectance from different thicknesses can be seen as a change in intensity on CCD.¹⁴⁹

glued to the transducer surface. The transducer surfaces were coated with biocompatible dextran. A thin layer of SiO_2 helps in the generation of waves for RIFS. The whole assembly was attached to a glass surface through which the sensor was “bottom illuminated” using a halogen source and a wheel monochromator. This light reflected by RIFS surfaces was detected using a CCD camera. The result was comparable to available fluorescent methods with no false negatives in the case of 96 well plates. This method can be applied to higher throughput screening like 1536-well plates.¹⁴⁴

In 2008, Ozkumur *et al.*, introduced a similar reflectance based interferometric detection method initially termed Spectral Reflectance Imaging Biosensor (SRIB) and recently renamed Interferometric Reflectance Imaging Sensor (IRIS) with a sensitivity comparable to an SPR sensor.

In this technique, in place of the white light source, a Laser/LED is used. SiO_2 is grown on a Si substrate for providing a platform for the attachment of molecular probes. The principle of spectroscopy is used to identify a change in optical thickness as seen in Figure 40. The light reflected from the substrate is detected by the CCD camera and the change in optical thickness is predicted based on interference patterns. They demonstrated the applicability of an SRIB by dynamically monitoring antigen antibody binding using 50 spots for each of four proteins consisting of BSA, human serum albumin, rabbit IgG, and protein G. An LOD of 19 ng/ml was achieved.¹⁴⁵ Later, they demonstrated a SRIB for the detection of DNA and proteins in microarray.¹⁴⁶

The direct detection of DNA hybridization and single-nucleotide mismatches was achieved using SRIB technique. The results were excellent as mismatches were identified in more than 97% of the samples.¹⁴⁷ Recently, a review on the applicability of SRIB in different areas of research has been published.¹⁴⁸

4.6 Integration and multiplexing in interferometry based devices

Compared to many other techniques, interferometry lends itself to integration on a chip, and thereby parallel detection schemes, more easily. Using standard microfabrication technology, waveguides can be fabricated so that they form the arms of an interferometer. One (or more) of the arms, works as the reference arm(s). Two configurations have mainly been used: the Mach Zehnder

interferometer and Young's Interferometer. In the former case, the input light, after passing through a common section of the waveguide is split into two parts using a "Y" junction, and after traversing through the sensing region of the waveguides, the light from the two arms is combined again using a similar junction (Figure 41). Since a sensing event leads to a phase change of the light in the sensing arm, the two waves interfere in a particular pattern.

In the case of Young's interferometer (YI) there is no Y-junction after passing through the sensing area, since the output light from reference and sensing arms interfere in free space and the pattern is picked up using a CCD detector. High sensitivity in the range of 10^{-6} to 10^{-8} RIU has been observed. Various materials like SiO_2 , Si_3N_4 , polymers, etc. are being used for their fabrication. It is quite obvious that the degree of phase change will depend on the length of the sensing arm and the fact that only single mode waveguides can be used.

Interferometers have demonstrated high sensitivity and stability due to inbuilt referencing which has led researchers to apply interferometers for multianalyte sensing. Ymeti *et al.*, 2002 demonstrated the first multichannel YI based immunosensor.¹⁵⁰ They fabricated the YI using

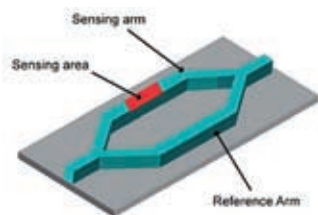


Figure 41: Mach-Zehnder interferometer integrated as waveguide.⁴¹

SiON technology and demonstrated a long term sensitivity of 2×10^{-7} RIU. They fabricated a 4 channel YI in such a way as to monitor the effects of the two channel pairs separately from the other. The distances between the channels were not the same. The Fast Fourier Transform output showed the presence of distinct peaks for different pairs of waveguides. This was modified later to a system which supported sensing from three channels, keeping the fourth as reference (Figure 42). Later, they fabricated 11 four channel YI on an optical chip and combined microfluidics to this multichannel YI.¹⁵¹ A refractive index resolution of 6×10^{-8} RIU was observed which was quite high compared to other label free sensing methods. Further, the utilization of microfluidics made it possible to get a stable output in only 4 seconds which, compared to a standard time of 100 seconds, was very significant. They further detected different viruses using specific antibodies as shown in Figure 42.¹⁵² The results showed the possibility of single virus detection and strengthened its feasibility for POC devices without extensive sample preparation steps.

Recently, Petrou *et al.*, (2010) fabricated a monolithic MZI array. They used a novel concept called Frequency-Resolved Mach-Zehnder Interferometry (FR-MZI) for detection. They integrated the light source and photodetectors on a chip, so as to avoid bulky optics, and thereby minimized the problem of light coupling. They developed an array of MZIs with individual light sources (LEDs) of different wavelengths and the output terminated at a single photodetector. A schematic depicting the MZI array is shown in Figure 43. Many sensors are connected in parallel for multiplexing. FR-MZI exploits the input frequency spectrum, offering high sensitivity robustness against phase ambiguities and loss of signal as seen in conventional single-wavelength MZI.¹⁵³

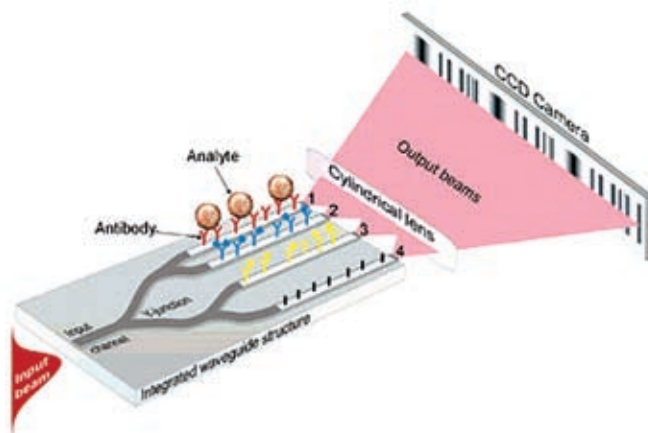


Figure 42: Representation of 4 channel YI showing different antibody immobilization at different channels.¹⁵²

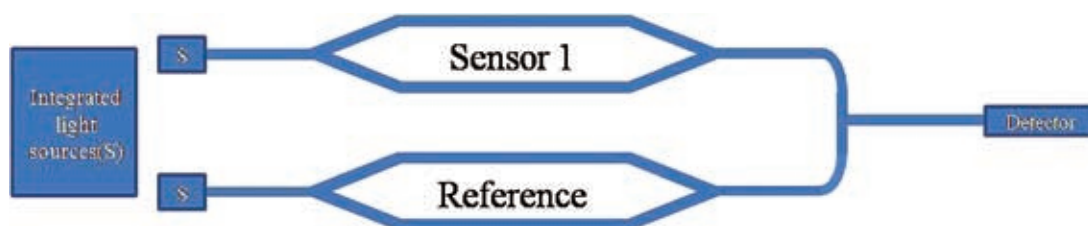


Figure 43: Representation of array of MZI for multiplexing. Adapted from Petrou *et al.*, 2010.

4.7 Ring resonators in integrated, multiplexed devices

Ring resonators have emerged as a class of compact sensors, by their ability to be integrated into small sizes without affecting the sensitivity of the device. This ability of integration and detection sensitivity down to single molecules has attracted the attention of many researchers towards the application of ring resonators in multiplexed sensing. The high sensitivity is achieved by the fact that the degree of interaction of light and the sample is not limited by the physical length of the sensing waveguide, but rather by the number of revolutions of light in the resonator. Further, ring resonators can be fabricated using different materials and microfabrication techniques that allow precise control of sizes. Etching and lithography techniques have helped make the surfaces smooth in order to increase the quality factor of ring resonators.

The initial application of microring resonators as optical biosensors was demonstrated by Vollmer *et al.*, in 2002 by detecting proteins.¹⁵⁴ This was closely followed by Ligler *et al.*,¹⁵⁵ who showed the possibility of multi analyte sensing by multiplexing 6 capillaries in a capillary based biosensor. Vollmer *et al.*, in 2003, demonstrated the application of multiplexed ring resonators to DNA detection using two microspheres. The spheres had unique resonant wavelengths so light could be coupled using a single waveguide and different oligonucleotides could be detected.¹⁵⁶ White *et al.*, (2006) fabricated and demonstrated the integration of 5 ring resonators together by using anti-resonant reflecting optical waveguide (ARROW) waveguide for coupling light and having a Liquid Core Ring Resonator (LCORR) for multiplex sensing.¹⁵⁷ Wang *et al.*, 2009 applied ring resonators to detect real time changes in the physical traits of live mammalian cells during cell adhesion and growth. They functionalized the ring resonator surface with an endothelial cell line (MS1) to detect the presence of two toxic chemicals, viz. sodium pentachlorophenate and aldicarb, in a solution which can be used for sensing toxic chemicals in water.⁴ This demonstrated the applicability of ring resonator based sensing to biophysical studies and to screening toxic chemicals.

Washburn *et al.*, (2009) demonstrated microring resonators for the detection of cancer biomarkers in a complex medium like serum.¹⁵⁸ Later in 2010, they took forward the concept to multiplexed sensing by demonstrating the applicability of label-free ring resonator biosensors for accurate immunoassays by detecting clinically relevant protein biomarkers. They simultaneously detected 5 protein biomarkers *i.e.* prostate specific antigen (PSA), α -fetoprotein (AFP), carcino-embryonic antigen (CEA), tumor necrosis factor- α (TNF- α), and interleukin-8 (IL-8) at a concentration of 10 ng/ml.¹⁵⁹

Iqbal *et al.*, 2010 presented a platform for multiple analyte sensing having an array of 32 ring resonators (8-controls and 24-sensing). They demonstrated multiplexing by using two DNA probes in a complex medium. They achieved a refractive index resolution of 7.6×10^{-7} and an LOD of 60 fM which was better than most other label-free sensor systems. A raster scan was performed to couple light to the input and detect it from the output side. The system used mirrors to detect light from different ring resonators on the array.¹⁶⁰ The system appeared to be functional, except for the fact that it requires complex optical and mechanical components for proper functioning.

A novel system was demonstrated by Carlborg *et al.*, in 2010 by integrating ring resonators with microfluidics for the detection of multiple analytes using multiple ring resonators on a single chip. They fabricated 7 ring resonators on the chip. Out of them, one was used for referencing to compensate for temperature variations.¹⁶¹ Six microfluidic channels were fabricated using PDMS. Light was coupled through a grating coupler and split by a splitter into 8 channels (6-sensing and 2-referencing). The output was detected simultaneously by an array of photodiodes. The cartridge was assembled in layers as shown in Figure 44. The LOD of the sensing system was 5×10^{-6} RIU, which was better than many previously reported Silicon nitride ring resonators. The system was robust due to the easy coupling of light, the adhesive bonding method and reference channels for the compensation of laser intensity or temperature fluctuations.

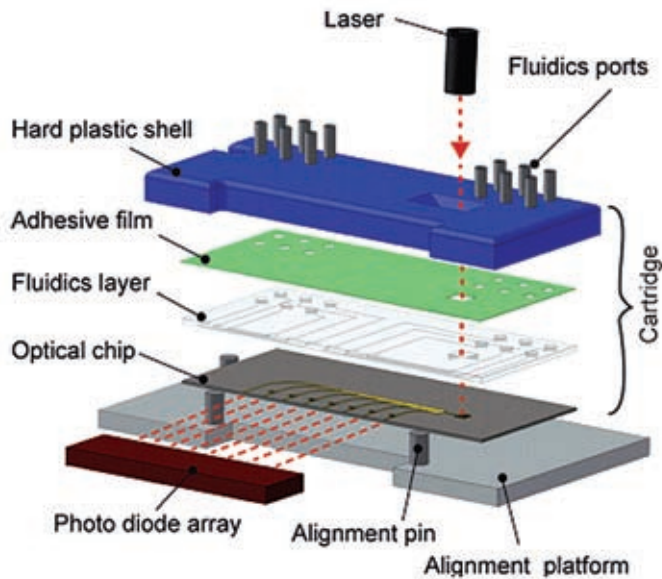


Figure 44: Different parts of the sensing system. At the base is the alignment platform and, above the platform is the optical chip consisting of ring resonators. The optical chip is covered with a hard plastic shell containing the microfluidics channels.¹⁶¹

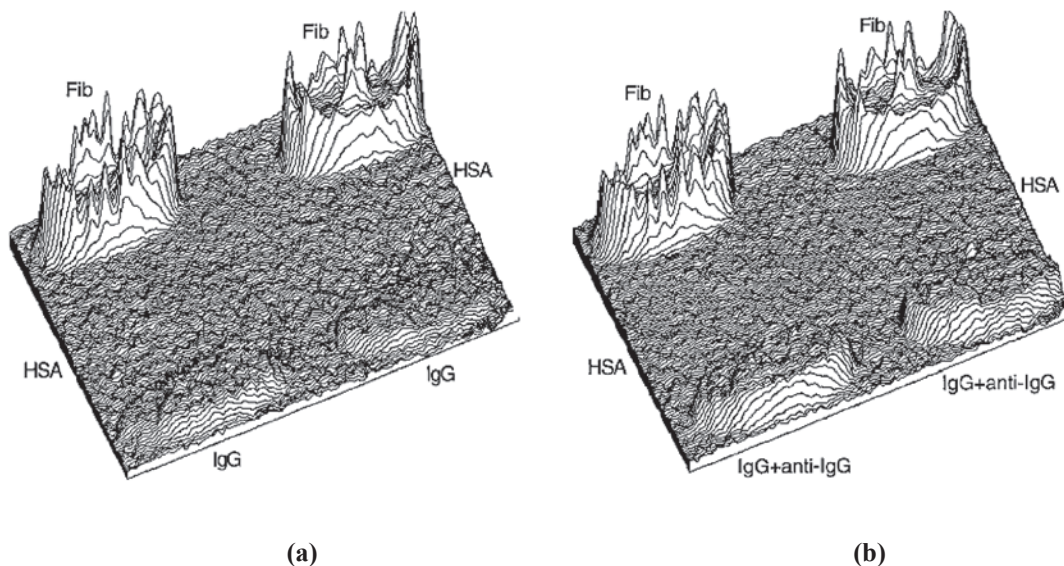


Figure 45: (a) Thickness of the substrate before incubation; (b) Thickness of the substrate after incubation of anti-IgG.¹⁶³

4.8 Ellipsometry

Ellipsometry can also be used in multiplexed and parallelized assays. The instrumentation with the required condition for a proper error-free result in imaging ellipsometry is well explained by Jin *et al.*, 1996.¹⁶² Since a simple TIRE-based technique is unlikely to be successful where multiple analytes have to be analyzed in parallel, researchers have developed Imaging Ellipsometry systems to overcome this limitation.

One of the first applications of biosensing using imaging ellipsometry was demonstrated for the detection of antigen-antibody complexes.¹⁶³ A silicon surface was taken and three types of antigens (Fibrinogen (Fib), Human serum albumin (HSA) and human immunoglobulin G (IgG)) were attached to the surface. Three rows of antigens were formed, each having two spots of the same antigen and about 3 mm in diameter. Various incubating steps were performed to

avoid nonspecific absorption. The ellipsometric image was taken before incubating in the antibody solution and the thickness profile was measured as shown in Figure 45a. After incubating in an Anti-IgG solution, the image was again taken as shown in Figure 45b. The difference in thickness is visible only at the row which contains IgG. The thickness change there is about 80%, compared to a change of less than 15% at other spots. Similar results were achieved with other antigen-antibody pairs.

Microfluidic array reactors are one of the major components of an ellipsometry setup. Using modern microfluidics techniques, many polymer-based flow cells are being fabricated which can increase the throughput of the technique.¹¹ The surface chemistry for interaction with the analyte or sample under study is also significant for increasing the sensitivity of the biosensor and for its prolonged use.

4.9 Miscellaneous

Many other unique and potentially powerful label-free optical detection schemes have been demonstrated for multiplexing. Cunningham *et al.*, 2002 demonstrated the applicability of narrow bandwidth guided mode resonant filters (GMRF) as biosensors.¹⁶⁴ They used this biosensor to perform a protein-protein affinity assay using a 96 well microplate. The setup was connected to the bottom of the microplate (Figure 46). White light was incident on the grating formed by the microwells and a shift in wavelength of the narrow band of resonant light which was dependent on the biomolecular interaction was detected.¹⁶⁵

Another fascinating design for multiplex biosensing was developed by Yan *et al.*, in 2009 using the principle of local evanescent array coupling (LEAC) (Figure 47). When a layer of biofilm is formed on the surface it causes a shift in a localized evanescent field. This shift of an evanescent field

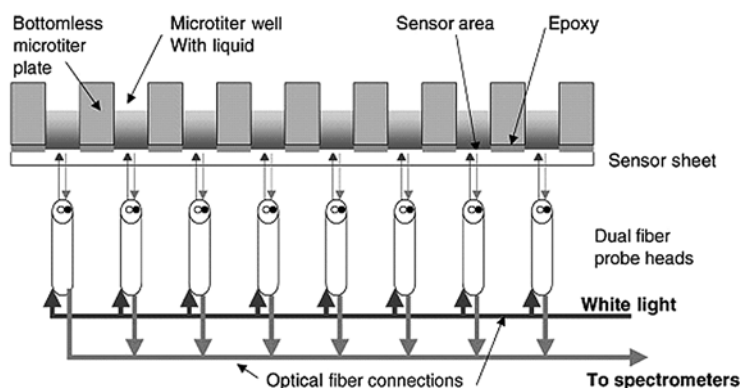


Figure 46: Guided mode resonance filter based biosensors.¹⁶⁶

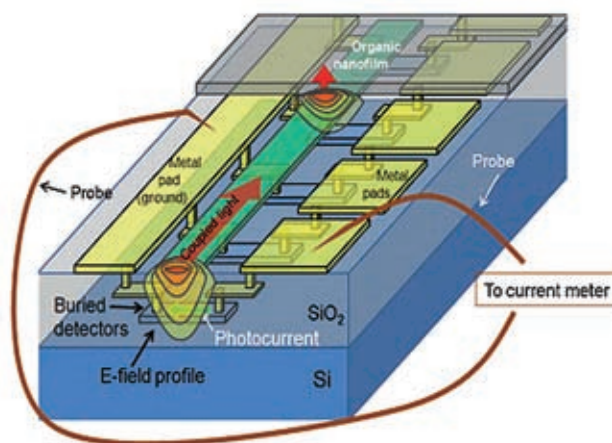


Figure 47: Schematic of LEAC biosensor.¹⁶⁷

in the vertical direction was detected by an array of buried photodetectors. As it is localized field redistribution, many different analytes could be detected at adjacent locations as the corresponding photodetector produces a current depending on the concentration of the binding analyte.¹⁶⁷

There are many other techniques which are being used to develop biosensor arrays, including photonic crystal^{168,169} arrays, and the amount of research in this area is evident from the fact that every alternate journal paper produced on biosensors deals with optical biosensors. In order to keep the length of this article within reasonable limits, those articles are not being discussed here. Readers of this article can find details about such techniques elsewhere, as in a recent review on label free photonic crystal biosensors.^{170,171}

5 The Future of Optical Techniques in Multiplexed, Parallelized, High Throughput Biosensing

The developments in the biosensing domain are being driven by two requirements: (1) The need for point of care (POC) diagnostics,^{52,172} (2) The need for high throughput laboratory based testing for a large number of samples and multiple target biomarkers.¹⁷³ The discovery of biomarkers as definitive diagnostics for various pathological and infective diseases is the causative factor for such requirements. As we have seen in the previous sections, the inherent advantages of optoelectronic sensing for biological markers have resulted in researchers and commercial organizations around the world competing to invent the most robust, sensitive and versatile biosensors. The possible impact of these sensors is tremendous, and the medical, public health and scientific advancements that may result from the development of appropriate biosensors is only to be imagined. The need for POC has been increasing and its applicability in different domains has been explored. In this context it is critical to have an idea of the latest research which is pushing the boundaries of sensing technologies to better sensitivities, higher specificities and hitherto unseen accuracies.

One of the obvious impacts would be felt in the area of software technology, which has been largely unexplored in this review article. A completely separate and equally long article can be written reviewing the impact of software on the parallelized biosensing domain. The impact starts right at the very early stages of development (in terms of simulation), continues through the control systems used in the driving electronics (FPGAs, etc.) and ends with the processing of acquired data to produce meaningful results, understandable

to ordinary human beings. In particular, with the help of optical simulation software, one can explore different designs for various configurations coming up with an optimized design and a prediction of expected results given an input. This translates to significant savings in terms of time and cost since various mistakes can be avoided without actually fabricating or experimenting using an actual device (e.g. Wan *et al.*, 2012¹⁷⁴).

It must be quite evident by now that the writers of this review consider SPR and LSPR techniques to be the most promising in terms of accuracy and integration in the short term. This is buttressed by the fact that quite a large number of research papers and reviews¹⁷⁵ have appeared in the last couple of years extending the boundaries of this sensing technique. Magneto Optic surface plasmon resonance that (MOSPR) technique is being developed and is based on increasing sensitivity by magneto plasmonic modulation.¹⁷⁶ This involves the excitation of surface plasmons along with a transverse magneto-optic Kerr effect (TMOKE) which only happens due to the presence of a magnetic field along the direction of the metal layers and perpendicular to the direction of the surface plasmon vector. This simultaneous excitement increases sensitivity.¹⁷⁷

In terms of LSPR, micro and nano-scaled structures like triangles and microholes are being exploited for short range SPR demonstrating the same sensitivity compared to surface-propagating plasmons and better than nanoparticle based surface plasmons.^{178–180} Nanotubes,¹⁸¹ cones,¹³⁰ and structures like dimers¹⁸² and trimers¹²⁸ have shown a novel plasmonic property which can be suitably tuned and used for sensing applications.

Another important aspect of sensor development involves surface chemistry which can have a profound effect on the lowering of the limit of detection. New techniques like the DNA-RNA antibody assay¹⁸³ and novel functionalization techniques¹⁸⁴ are examples of scientific endeavor in this direction. The issue of surface functionalization is closely related to surface fabrication which now leverages heavily on the development of novel microfabrication techniques like soluble substrate technology for producing structures like 'graticles' which can be directly used as surfaces for SPR imaging.¹⁸⁵ Other techniques including Inclined nanolithography,¹⁸⁶ localized oblique angle deposition,¹⁸⁷ near field guided nanopatterning,¹⁸⁸ templated techniques¹⁸⁹ electrochemical deposition by tapping mode atomic force microscopy¹⁹⁰ are being explored to create better surfaces on substrates for SPR based sensing. Many groups are also looking in to functionalization by dendrimers to increase the surface area for sensing.¹⁹¹

Yet another important development is where various detection techniques are being merged to provide higher accuracy/sensitivity/specificity. Merging angle interrogation and wavelength interrogation to take advantage of the benefits of high sensitivity and simple geometry¹⁹² is a simple example of this development. A more complex example involves the merging of SPR and mass spectroscopy. This utilizes the advantages of real time, kinematics study and the quantification of biomolecules by SPR and the elucidation of structural features by Mass Spectrometry (MS). It has found application in fields like proteome analysis¹⁹³ and miniaturized diagnostics.¹⁹⁴ They have been applied in microarray formats for multiplexed applications to meet the demand of upcoming “-omics” revolution.

It may be envisaged that in the near future POC diagnostics will attain fM sensitivity and proper sample preparation will be a key factor in accurate diagnostics. In this domain, further developments in microfluidics will play a key role, and so will sampling technologies. One of the major roles of microfluidics (simulation and hardware) will be in “focusing” the target analytes onto the sensing surfaces thereby increasing molecular capture rates.

Finally, in summary, in the view of the authors of this review, the possible domain of optical biosensing, both in terms of single analyte or multi-analyte sensing, is only explored partially and has ample scope for researchers to engage in research and development for cheaper, more sensitive, more specific and more accurate sensors.

Received 9 March 2012.

References

- Clark, L.C. and Lyons, C. “Electrode Systems For Continuous Monitoring In Cardiovascular Surgery.” *Annals of the New York Academy of Sciences* **102**, 29–45 (1962).
- Piehler, J., Brecht, A., Gauglitz, G., Zerlin, M., Maul, C., Thiericke, R. and Grabley, S. “Label-free monitoring of DNA-ligand interactions.” *Analytical Biochemistry* **249**, 94–102 (1997).
- Sawata, S., Kai, E., Ikebukuro, K., Iida, T., Honda, T. and Karube, I. “Application of peptide nucleic acid to the direct detection of deoxyribonucleic acid amplified by polymerase chain reaction.” *Biosensors and Bioelectronics* **14**, 397–404 (1999).
- Wang, S., Ramachandran, A. and Ja, S. “Integrated microring resonator biosensors for monitoring cell growth and detection of toxic chemicals in water.” *Biosensors & Bioelectronics* **24**, 3061–3066 (2009).
- Polster, J. “Simultaneous determination of penicillin and ampicillin by spectral fibre-optical enzyme optodes and multivariate data analysis based on transient signals obtained by flow injection analysis.” *Talanta* **42**, 2065–2072 (1995).
- Sai, V., Kundu, T. and Mukherji, S. “Novel U-bent fiber optic probe for localized surface plasmon resonance based biosensor.” *Biosensors & Bioelectronics* **24**, 2804–2809 (2009).
- Thévenot, D.R., Toth, K., Durst, R.A. and Wilson, G.S. “Electrochemical biosensors: recommended definitions and classification.” *Biosensors and Bioelectronics* **16**, 121–131 (2001).
- Fan, X., White, I.M., Shopova, S.I., Zhu, H., Suter, J.D. and Sun, Y. “Sensitive optical biosensors for unlabeled targets: a review.” *Analytica Chimica Acta* **620**, 8–26 (2008).
- Arlett, J.L., Myers, E.B. and Roukes, M.L. “Comparative advantages of mechanical biosensors.” *Nature Nanotechnology* **6**, 203–215 (2011).
- Catimel, B., Rothacker, J., Catimel, J., Faux, M., Ross, J., Connolly, L., Clippingdale, A., Burgess, A.W. and Nice, E. “Biosensor-based micro-affinity purification for the proteomic analysis of protein complexes.” *Journal of Proteome Research* **4**, 1646–1656.
- Rivet, C., Lee, H., Hirsch, A., Hamilton, S. and Lu, H. “Microfluidics for medical diagnostics and biosensors.” *Chemical Engineering Science* **66**, 1490–1507 (2011).
- Shuman, C.F., Hämäläinen, M.D. and Danielson, U.H. “Kinetic and thermodynamic characterization of HIV-1 protease inhibitors.” *Journal of Molecular Recognition* **17**, 106–119.
- Cooper, M.A. “Optical biosensors in drug discovery.” *Nature Reviews Drug Discovery* **1**, 515–528 (2002).
- Vo-Dinh, T. and Cullum, B. “Biosensors and biochips: advances in biological and medical diagnostics.” *Fresenius’ Journal of Analytical Chemistry* **366**, 540–551 (2008).
- Rodriguez-Mozaz, S., Lopez de Alda, M.J. and Barceló, D. “Biosensors as useful tools for environmental analysis and monitoring.” *Analytical and Bioanalytical Chemistry* **386**, 1025–1041 (2006).
- Gauglitz, G. “Optical detection methods for combinatorial libraries.” *Current Opinion in Chemical Biology* **4**, 351–355 (2000).
- Ivnitski, D., Abdel-Hamid, I., Atanasov, P. and Wilkins, E. “Biosensors for detection of pathogenic bacteria.” *Biosensors and Bioelectronics* **14**, 599–624 (1999).
- Dougherty, G.M., Clague, D.S. and Miles, R.R. “Field-capable biodetection devices for homeland security missions.” *Proceedings of SPIE* **6540**, 654016-654016-10 (2007).
- Nielsen, U.B. and Geierstanger, B.H. “Multiplexed sandwich assays in microarray format.” *Journal of Immunological Methods* **290**, 107–120 (2004).
- Sloan, J.H., Ackermann, B.J., O’Dell, M., Bowsher, R.R., Dean, R.A. and Konrad, R.J. “Development of a novel radioimmunoassay to detect autoantibodies to amyloid beta peptides in the presence of a cross-reactive therapeutic antibody.” *Journal of Pharmaceutical and Biomedical Analysis* **56**, 1029–1034 (2011).

21. Anderson, G.P. and Nerurkar, N.L. "Improved fluoroimmunoassays using the dye Alexa Fluor 647 with the RAPTOR, a fiber optic biosensor." *Journal of Immunological Methods* **271**, 17–24 (2002).
22. Divsar, F. and Ju, H. "Electrochemiluminescence detection of near single DNA molecules by using quantum dots-dendrimer nanocomposites for signal amplification." *Chemical Communications (Cambridge, England)* **47**, 9879–9781 (2011).
23. Huber, W. and Mueller, F. "Biomolecular interaction analysis in drug discovery using surface plasmon resonance technology." *Current Pharmaceutical Design* **12**, 3999–4021 (2006).
24. Rapp, B.E., Gruhl, F.J. and Länge, K. "Biosensors with label-free detection designed for diagnostic applications." *Analytical And Bioanalytical Chemistry* **398**, 2403–2412 (2010).
25. Cunningham, B. "Label-Free Biosensors Techniques and Applications." 3–4 (Cambridge University Press: 2009).
26. Perkel, J. "Who Needs Labels?: Macromolecular Interaction Sans Labels." *Science* **325**, 1561–1565 (2009).
27. Gauglitz, G. "Direct optical detection in bioanalysis: an update." *Analytical And Bioanalytical Chemistry* **398**, 2363–2372 (2010).
28. Sai, V., Kundu, T., Deshmukh, C., Titus, S., Kumar, P. and Mukherji, S. "Label-free fiber optic biosensor based on evanescent wave absorbance at 280 nm." *Sensors and Actuators B* **143**, 724–730 (2010).
29. Gupta, B.D., Dodeja, H. and Tomar, A.K. "Fibre-optic evanescent field absorption sensor based on a U-shaped probe." *Optical and Quantum Electronics* **28**, 1629–1639 (1996).
30. Khijwania, S. and Gupta, B. "Maximum achievable sensitivity of the fiber optic evanescent field absorption sensor based on the U-shaped probe." *Optics Communications* **175**, 135–137 (2000).
31. Verma, R.K., Sharma, A.K. and Gupta, B.D. "Modeling of Tapered Fiber-Optic Surface Plasmon Resonance Sensor With Enhanced Sensitivity." *IEEE Photonics Technology Letters* **19**, 1786–1788 (2007).
32. Bharadwaj, R., Sai, V., Thakare, K., Dhawangale, A., Kundu, T., Titus, S., Verma, P.K. and Mukherji, S. "Evanescent wave absorbance based fiber optic biosensor for label-free detection of E. coli at 280 nm wavelength." *Biosensors & Bioelectronics* **26**, 3367–3370 (2011).
33. Liedberg, B., Nylander, C. and Lunström, I. "Surface plasmon resonance for gas detection and biosensing." *Sensors and Actuators* **4**, 299–304 (1983).
34. Ho, H.P., Lam, W.W. and Wu, S.Y. "Surface plasmon resonance sensor based on the measurement of differential phase." *Review of Scientific Instruments* **73**, 3534–3539 (2002).
35. Toyama, S., Doumae, N., Shoji, A. and Ikariyama, Y. "Design and fabrication of a waveguide-coupled prism device for surface plasmon resonance sensor." *Sensors and Actuators B: Chemical* **65**, 32–34 (2000).
36. Kuo, W. and Chang, C. "Phase detection properties of grating-coupled surface plasmon resonance sensors." *Optics Express* **18**, 19656–19664 (2010).
37. Sabban, S. "Development of an in vitro model system for studying the interaction of Equus caballus IgE with its high-affinity FcεRI receptor." *Department of Molecular Biology and biotechnology, The University of Sheffield* (2011) <<http://etheses.whiterose.ac.uk/2040/>>
38. Hutter, E. and Fendler, J.H. "Exploitation of Localized Surface Plasmon Resonance." *Advanced Materials* **16**, 1685–1706 (2004).
39. Prabhakar, A. and Mukherji, S. "C-shaped embedded polymer waveguide for evanescent field absorption based lab on a chip biosensor." *2010 International Conference on Systems in Medicine and Biology* 67–70 (2010). doi: 10.1109/ICSMB.2010.5735347.
40. Satija, J., Bharadwaj, R., Sai, V. and Mukherji, S. "Emerging use of nanostructure films containing capped gold nanoparticles in biosensors." *Nanotechnology, Science and Applications* **3**, 171–188 (2010).
41. Washburn, A.L. and Bailey, R.C. "Photonics-on-a-chip: recent advances in integrated waveguides as enabling detection elements for real-world, lab-on-a-chip biosensing applications." *The Analyst* **136**, 227–236 (2011).
42. Gauglitz, G. "Multiple reflectance interference spectroscopy measurements made in parallel for binding studies." *Review of Scientific Instruments* **76**, 062224–062224-10 (2005).
43. Niu, Y. and Jin, G. "Protein microarray biosensors based on imaging ellipsometry techniques and their applications." *Protein & Cell* **2**, 445–455 (2011).
44. Chen, Y.Y., Wang, Z.H., Meng, Y.H. and Jin, G. "Biosensor with total internal reflection imaging ellipsometry." *International Journal of Nanotechnology* **4**, 171–178 (2007).
45. Jin, G. "Development of biosensor based on imaging ellipsometry and its applications." 78750E-78750E-7 (2011). doi:10.1117/12.871981.
46. Shvets, V.A., Spesivtsev, E.V., Rykhliitskii, S.V. and Mikhailov, N.N. "Ellipsometry as a high-precision technique for subnanometer-resolved monitoring of thin-film structures." *Nanotechnologies in Russia* **4**, 201–214 (2009).
47. Westphal, P. and Bornmann, A. "Biomolecular detection by surface plasmon enhanced ellipsometry." *Sensors And Actuators* **84**, 278–282 (2002).
48. Rasing, T., Hsiung, H., Shen, Y. and Kim, M. "Ellipsometry study of two-dimensional phase transitions." *Physical Review A* **37**, 2732–2735 (1988).
49. Kim, M.W., Peiffer, D.G., Chen, W., Hsiung, H., Rasing, T. and Shen, Y.R. "Polymer concentration profile near a liquid-solid interface: evanescent wave ellipsometry study." *Macromolecules* **22**, 2682–2685 (1989).
50. Poksinski, M. and Arwin, H. "In situ monitoring of metal surfaces exposed to milk using total internal reflection ellipsometry." *Sensors and Actuators B: Chemical* **94**, 247–252 (2003).

51. Arwin, H., Poksinski, M. and Johansen, K. "Total Internal Reflection Ellipsometry: Principles and Applications." *Applied Optics* **43**, 3028 (2004).
52. Gubala, V., Harris, L.F., Ricco, A.J., Tan, M.X. and Williams, D.E. "Point of care diagnostics: status and future." *Analytical chemistry* **84**, 487–515 (2012).
53. Gonzalez, A.B.K. "Silicon photonic biosensors for high innovative point-of-care diagnostic platforms." *2011 ICO International Conference on Information Photonics* **2**, 1–2 (2011).
54. Kley, E.-B. "E-beam lithography: a suitable technology for fabrication of high-accuracy 2D and 3D surface profiles." *Proceedings of SPIE* **2640**, 71–80 (1995).
55. Hruby, J. "LIGA Technologies and Applications." *MRS Bulletin* **26**, 337–340 (2011).
56. Prabhakar, A. and Mukherji, S. "Microfabricated polymer chip with integrated U-bend waveguides for evanescent field absorption based detection." *Lab on a Chip* **10**, 748–754 (2010).
57. Fontana, E. "A novel gold-coated multimode fiber sensor." *IEEE Transactions on Microwave Theory and Techniques* **50**, 82–87 (2002).
58. Kim, K.T., Song, H.S., Mah, J.P., Hong, K.B., Im, K., Baik, S.-J. and Yoon, Y.-I. "Hydrogen Sensor Based on Palladium Coated Side-Polished Single-Mode Fiber." *IEEE Sensors Journal* **7**, 1767–1771 (2007).
59. Jorgenson, R.C. and Yee, S.S. "A fiber-optic chemical sensor based on surface plasmon resonance." *Sensors and Actuators B: Chemical* **12**, 213–220 (1993).
60. Díez, A., Andrés, M.V. and Cruz, J.L. "In-line fiber-optic sensors based on the excitation of surface plasma modes in metal-coated tapered fibers." *Sensors and Actuators B: Chemical* **73**, 95–99 (2001).
61. Kurihara, K., Ohkawa, H., Iwasaki, Y., Niwa, O., Tobita, T. and Suzuki, K. "Fiber-optic conical microsensors for surface plasmon resonance using chemically etched single-mode fiber." *Analytica Chimica Acta* **523**, 165–170 (2004).
62. Masson, J.-F., Kim, Y.-C., Obando, L.A., Peng, W. and Booksh, K.S. "Fiber-Optic Surface Plasmon Resonance Sensors in the Near-Infrared Spectral Region." *Applied Spectroscopy* **60**, 1241–1246 (2006).
63. Jha, R., Verma, R.K. and Gupta, B.D. "Surface Plasmon Resonance-Based Tapered Fiber Optic Sensor: Sensitivity Enhancement by Introducing a Teflon Layer Between Core and Metal Layer." *Plasmonics* **3**, 151–156 (2008).
64. Srivastava, S.K. and Gupta, B.D. "A Multitapered Fiber-Optic SPR Sensor With Enhanced Sensitivity." *IEEE Photonics Technology Letters* **23**, 923–925 (2011).
65. Geng, Z., Li, Q., Wang, W. and Li, Z. "PDMS prism-glass optical coupling for surface plasmon resonance sensors based on MEMS technology." *Science China Information Sciences* **53**, 2144–2158 (2010).
66. Chien, W.-Y., Khalid, M.Z., Hoa, X.D. and Kirk, A.G. "Monolithically integrated surface plasmon resonance sensor based on focusing diffractive optic element for optofluidic platforms." *Sensors and Actuators B: Chemical* **138**, 441–445 (2009).
67. Hoa, X.D., Kirk, A.G. and Tabrizian, M. "Towards integrated and sensitive surface plasmon resonance biosensors: a review of recent progress." *Biosensors & Bioelectronics* **23**, 151–160 (2007).
68. Suzuki, A., Kondoh, J. and Matsui, Y. "Development of novel optical waveguide surface plasmon resonance (SPR) sensor with dual light emitting diodes." *Sensors and Actuators B: Chemical* **106**, 383–387 (2005).
69. Huang, Z.-he, Hou, J., Peng, Y. and Chen, J.-bao. "Surface plasmon resonance sensor based on supercontinuum source." *Proc. SPIE* **8191** 81910Z-81910Z-5 (2011). doi:10.1117/12.900237.
70. Melendez, J., Carr, R., Bartholomew, D.U., Kukanskis, K., Elkind, J., Yee, S., Furlong, C. and Woodbury, R. "A commercial solution for surface plasmon sensing." *Sensors and Actuators B: Chemical* **35**, 212–216 (1996).
71. Chinowsky, T., Quinn, J., Bartholomew, D., Kaiser, R. and Elkind, J. "Performance of the Spreeta 2000 integrated surface plasmon resonance affinity sensor." *Sensors and Actuators B: Chemical* **91**, 266–274 (2003).
72. Elkind, J., Stimpson, D., Strong, A.A., Bartholomew, D. and Melendez, J. "Integrated analytical sensors: the use of the TISPR-1 as a biosensor." *Sensors and Actuators B: Chemical* **54**, 182–190 (1999).
73. Thagard, P. "Pathways to Biomedical Discovery." *Philosophy of Science* **70**, 235–254 (2003).
74. Seidel, M. and Niessner, R. "Automated analytical microarrays: a critical review." *Analytical And Bioanalytical Chemistry* **391**, 1521–1544 (2008).
75. Löfås, S., Malmqvist, M., Rönnerberg, I., Stenberg, E., Liedberg, B. and Lundström, I. "Bioanalysis with surface plasmon resonance." *Sensors and Actuators B: Chemical* **5**, 79–84 (1991).
76. Nenninger, G., Clendenning, J., Furlong, C. and Yee, S. "Reference-compensated biosensing using a dual-channel surface plasmon resonance sensor system based on a planar lightpipe configuration." *Sensors and Actuators B: Chemical* **51**, 38–45 (1998).
77. Homola, J., Lu, H.B. and Yee, S.S. "Dual-channel surface plasmon resonance sensor with spectral discrimination of sensing channels using dielectric overlayer." *Electronics Letters* **35**, 1105–1106 (1999).
78. Homola, J., Lu, H.B., Nenninger, G.G., Dostálek, J. and Yee, S.S. "A novel multichannel surface plasmon resonance biosensor." *Sensors and Actuators B: Chemical* **76**, 403–410 (2001).
79. Homola, J., Vaisocherová, H., Dostálek, J. and Piliarik, M. "Multi-analyte surface plasmon resonance biosensing." *Methods* **37**, 26–36 (2005).
80. Boozer, C., Kim, G., Cong, S., Guan, H. and Londergan, T. "Looking towards label-free biomolecular interaction analysis in a high-throughput format: a review of new surface plasmon resonance technologies." *Current Opinion In Biotechnology* **17**, 400–405 (2006).

81. Huang, H. and Chen, Y. "Label-free reading of microarray-based proteins with high throughput surface plasmon resonance imaging." *Biosensors & Bioelectronics* **22**, 644–648 (2006).
82. Dong, Y., Wilkop, T., Xu, D., Wang, Z. and Cheng, Q. "Microchannel chips for the multiplexed analysis of human immunoglobulin G-antibody interactions by surface plasmon resonance imaging." *Analytical And Bioanalytical Chemistry* **390**, 1575–1583 (2008).
83. Piliarik, M., Vaisocherová, H. and Homola, J. "A new surface plasmon resonance sensor for high-throughput screening applications." *Biosensors & Bioelectronics* **20**, 2104–2110 (2005).
84. Piliarik, M. and Homola, J. "Self-referencing SPR imaging for most demanding high-throughput screening applications." *Sensors and Actuators B: Chemical* **134**, 353–355 (2008).
85. Piliarik, M., Párová, L. and Homola, J. "High-throughput SPR sensor for food safety." *Biosensors & Bioelectronics* **24**, 1399–1404 (2009).
86. Piliarik, M., Bocková, M. and Homola, J. "Surface plasmon resonance biosensor for parallelized detection of protein biomarkers in diluted blood plasma." *Biosensors & Bioelectronics* **26**, 1656–1661 (2010).
87. Krishnamoorthy, G., Carlen, E.T., Kohlheyer, D., Schasfoort, R.B.M. and van den Berg, A. "Integrated electrokinetic sample focusing and surface plasmon resonance imaging system for measuring biomolecular interactions." *Analytical Chemistry* **81**, 1957–1963 (2009).
88. Spehar, A.-M., Koster, S., Linder, V., Kulmala, S., de Rooij, N.F., Verpoorte, E., Sigrist, H. and Thormann, W. "Electrokinetic characterization of poly(dimethylsiloxane) microchannels." *Electrophoresis* **24**, 3674–3678 (2003).
89. Satyanarayana, S., Karnik, R.N. and Majumdar, A. "Stamp-and-stick room-temperature bonding technique for microdevices." *Journal of Microelectromechanical Systems* **14**, 392–399 (2005).
90. Krishnamoorthy, G., Carlen, E.T., Bomer, J.G., Wijnperlé, D., DeBoer, H.L., Van Den Berg, A. and Schasfoort, R.B.M. "Electrokinetic label-free screening chip: a marriage of multiplexing and high throughput analysis using surface plasmon resonance imaging." *Lab on a Chip* **10**, 986–990 (2010).
91. Dostalek, J. and Vaisocherov, H. "Multichannel surface plasmon resonance biosensor with wavelength division multiplexing." *Sensors and Actuators B: Chemical* **108**, 758–764 (2005).
92. Fernández, F., Hegnerová, K., Piliarik, M., Sanchez-Baeza, F., Homola, J. and Marco, M.-P. "A label-free and portable multichannel surface plasmon resonance immunosensor for on site analysis of antibiotics in milk samples." *Biosensors & Bioelectronics* **26**, 1231–1238 (2010).
93. Telezhnikova, O. and Homola, J. "New approach to spectroscopy of surface plasmons." *Optics Letters* **31**, 3339–3341 (2006).
94. Piliarik, M., Vala, M., Tichý, I. and Homola, J. "Compact and low-cost biosensor based on novel approach to spectroscopy of surface plasmons." *Biosensors & Bioelectronics* **24**, 3430–3435 (2009).
95. Berger, V., Gauthier-Lafaye, O. and Costard, E. "Fabrication of a 2D photonic bandgap by a holographic method." *Electronics Letters* **33**, 425–426 (1997).
96. Xia, Y. and Whitesides, G.M. "Soft Lithography." *Angewandte Chemie International Edition* **37**, 550–575 (1998).
97. Dostálek, J., Homola, J. and Miler, M. "Rich information format surface plasmon resonance biosensor based on array of diffraction gratings." *Sensors and Actuators B: Chemical* **107**, 154–161 (2005).
98. Akowuah, E.K., Gorman, T., Haxha, S. and Oliver, J.V. "Dual channel planar waveguide surface plasmon resonance biosensor for an aqueous environment." *Optics Express* **18**, 24412–24422 (2010).
99. Springer, T., Piliarik, M. and Homola, J. "Surface plasmon resonance sensor with dispersionless microfluidics for direct detection of nucleic acids at the low femtomole level." *Sensors and Actuators B: Chemical* **145**, 588–591 (2010).
100. Olkhov, R.V. and Shaw, A.M. "Label-free antibody-antigen binding detection by optical sensor array based on surface-synthesized gold nanoparticles." *Biosensors & Bioelectronics* **23**, 1298–1302 (2008).
101. Olkhov, R.V. and Shaw, A.M. "Quantitative label-free screening for antibodies using scattering biophotonic microarray imaging." *Analytical Biochemistry* **396**, 30–35 (2010).
102. Ouellet, E., Lausted, C., Lin, T., Yang, C.W.T., Hood, L. and Lagally, E.T. "Parallel microfluidic surface plasmon resonance imaging arrays." *Lab on a Chip* **10**, 581–588 (2010).
103. Unger, M.A., Chou, H.-P., Thorsen, T., Scherer, A. and Quake, S.R. "Monolithic Microfabricated Valves and Pumps by Multilayer Soft Lithography." *Science* **288**, 113–116 (2000).
104. Wang, J., Luo, Y., Zhang, B., Chen, M., Huang, J., Zhang, K., Gao, W., Fu, W., Jiang, T. and Liao, P. "Rapid label-free identification of mixed bacterial infections by surface plasmon resonance." *Journal of Translational Medicine* **9**:85, 1–9 (2011).
105. Lee, H.H., Smoot, J., McMurray, Z., Stahl, D.A. and Yager, P. "Recirculating flow accelerates DNA microarray hybridization in a microfluidic device." *Lab on a chip* **6**, 1163–1170 (2006).
106. Homola, J., Dostálek, J., Chen, S., Rasooly, A., Jiang, S. and Yee, S.S. "Spectral surface plasmon resonance biosensor for detection of staphylococcal enterotoxin B in milk." *International Journal Of Food Microbiology* **75**, 61–69 (2002).
107. Sutapun, B., Somboonkaew, A., Amrit, R., Houngkamhang, N. and Sriksirin, T. "A multichannel surface plasmon resonance sensor using a new spectral readout system without moving optics." *Sensors and Actuators B: Chemical* **156**, 312–318 (2011).

108. Bardin, F., Bellemain, A., Roger, G. and Canva, M. "Surface plasmon resonance spectro-imaging sensor for biomolecular surface interaction characterization." *Biosensors & Bioelectronics* **24**, 2100–2105 (2009).
109. Pedersen, H.C. and Thirstrup, C. "Design of near-field holographic optical elements by grating matching." *Applied Optics* **43**, 1209–1215 (2004).
110. Thirstrup, C., Zong, W., Borre, M., Neff, H., Pedersen, H. and Holzhueter, G. "Diffractive optical coupling element for surface plasmon resonance sensors." *Sensors and Actuators B: Chemical* **100**, 298–308 (2004).
111. Piliarik, M., Vaisocherova, H. and Homola, J. "Towards parallelized surface plasmon resonance sensor platform for sensitive detection of oligonucleotides." *Sensors and Actuators B: Chemical* **121**, 187–193 (2007).
112. Chen, S., Su, Y., Hsiu, F., Tsou, C. and Chen, Y. "Surface plasmon resonance phase-shift interferometry: Real-time DNA microarray hybridization analysis." *Journal of Biomedical Optics* **10**, 034005 (2005).
113. Halpern, A.R., Chen, Y., Corn, R.M. and Kim, D. "Surface plasmon resonance phase imaging measurements of patterned monolayers and DNA adsorption onto microarrays." *Analytical Chemistry* **83**, 2801–2806 (2011).
114. Säfsten, P., Klakamp, S.L., Drake, A.W., Karlsson, R. and Myszka, D.G. "Screening antibody-antigen interactions in parallel using Biacore A100." *Analytical Biochemistry* **353**, 181–190 (2006).
115. Situ, C., Mooney, M.H., Elliott, C.T. and Buijs, J. "Advances in surface plasmon resonance biosensor technology towards high-throughput, food-safety analysis." *TrAC Trends in Analytical Chemistry* **29**, 1305–1315 (2010).
116. Abdiche, Y.N., Lindquist, K.C., Pinkerton, A., Pons, J. and Rajpal, A. "Expanding the ProteOn XPR36 biosensor into a 36-ligand array expedites protein interaction analysis." *Analytical Biochemistry* **411**, 139–151 (2011).
117. Nahshol, O., Bronner, V., Notcovich, A., Rubrecht, L., Laune, D. and Bravman, T. "Parallel kinetic analysis and affinity determination of hundreds of monoclonal antibodies using the ProteOn XPR36." *Analytical Biochemistry* **383**, 52–60 (2008).
118. Prabhakar, A. and Mukherji, S. "A novel C-shaped, gold nanoparticle coated, embedded polymer waveguide for localized surface plasmon resonance based detection." *Lab on a Chip* **10**, 3422–3425 (2010).
119. Dick, L.A., McFarland, A.D., Haynes, C.L. and Van Duyne, R.P. "Metal Film over Nanosphere (MFON) Electrodes for Surface-Enhanced Raman Spectroscopy (SERS): Improvements in Surface Nanostructure Stability and Suppression of Irreversible Loss." *The Journal of Physical Chemistry B* **106**, 853–860 (2002).
120. Ma, W., Yang, H., Wang, W., Gao, P. and Yao, J. "Ethanol vapor sensing properties of triangular silver nanostructures based on localized surface plasmon resonance." *Sensors (Basel, Switzerland)* **11**, 8643–8653 (2011).
121. Petryayeva, E. and Krull, U.J. "Localized Surface Plasmon Resonance: Nanostructures, Bioassays and Biosensing—A Review." *Analytica Chimica Acta* **706**, 8–24 (2011).
122. Hicks, E.M., Zhang, X., Zou, S., Lyandres, O., Spears, K.G., Schatz, G.C. and Van Duyne, R.P. "Plasmonic properties of film over nanowell surfaces fabricated by nanosphere lithography." *The Journal of Physical Chemistry. B* **109**, 22351–22358 (2005).
123. Haynes, C.L. and Van Duyne, R.P. "Nanosphere Lithography: A Versatile Nanofabrication Tool for Studies of Size-Dependent Nanoparticle Optics." *The Journal of Physical Chemistry B* **105**, 5599–5611 (2001).
124. Watkins, R.E.J., Rockett, P., Thoms, S., Clampitt, R. and Syms, R. "Focused ion beam milling." *Vacuum* **36**, 961–967 (1986).
125. Piner, R.D., Zhu, J., Xu, F., Hong, S. and Mirkin, C.A. "Dip-Pen Nanolithography." *Science* **283**, 661–663 (1999).
126. Henzie, J., Lee, J., Lee, M.H., Hasan, W. and Odom, T.W. "Nanofabrication of plasmonic structures." *Annual Review of Physical Chemistry* **60**, 147–165 (2009).
127. Shin, Y.-B., Lee, J.-M., Park, M.-R., Kim, M.-G., Chung, B.H., Pyo, H.-B. and Maeng, S. "Analysis of recombinant protein expression using localized surface plasmon resonance (LSPR)." *Biosensors & Bioelectronics* **22**, 2301–2307 (2007).
128. Teo, S.L., Lin, V.K., Marty, R., Large, N., Llado, E.A., Arbouet, A., Girard, C., Aizpurua, J., Tripathy, S. and Mlayah, A. "Gold nanoring trimers: a versatile structure for infrared sensing." *Optics Express* **18**, 22271–22282 (2010).
129. Zhu, S. and Zhou, W. "Optical properties of pentagram nanostructures based on localized surface plasmon resonance." *Journal of Optics* **40**, 65–70 (2011).
130. Wu, W., Hu, M., Ou, F.S., Li, Z. and Williams, R.S. "Cones fabricated by 3D nanoimprint lithography for highly sensitive surface enhanced Raman spectroscopy." *Nanotechnology* **21**, 255502 (2010).
131. Tang, J., Ou, F.S., Kuo, H.P., Hu, M., Stickle, W.F., Li, Z. and Williams, R.S. "Silver-coated Si nanoglass as highly sensitive surface-enhanced Raman spectroscopy substrates." *Applied Physics A* **96**, 793–797 (2009).
132. Lesuffleur, A., Im, H., Lindquist, N.C., Lim, K.S. and Oh, S.-H. "Laser-illuminated nanohole arrays for multiplex plasmonic microarray sensing." *Optics Express* **16**, 219–224 (2008).
133. Ebbesen, T.W., Lezec, H.J., Ghaemi, H.F., Thio, T. and Wolff, P.A. "Extraordinary optical transmission through sub-wavelength hole arrays." *Nature* **391**, 667–669 (1998).
134. Martín-Moreno, L., García-Vidal, F., Lezec, H., Pellerin, K., Thio, T., Pendry, J. and Ebbesen, T. "Theory of Extraordinary Optical Transmission through Subwavelength Hole Arrays." *Physical Review Letters* **86**, 1114–1117 (2001).
135. Brolo, A.G., Gordon, R., Leathem, B. and Kavanagh, K.L. "Surface Plasmon Sensor Based on the Enhanced Light Transmission through Arrays of Nanoholes in Gold Films." *Langmuir* **20**, 4813–4815 (2004).

136. De Leebeek, A., Kumar, L.K.S., de Lange, V., Sinton, D., Gordon, R. and Brolo, A.G. "On-chip surface-based detection with nanohole arrays." *Analytical Chemistry* **79**, 4094–4100 (2007).
137. Ji, J., O'Connell, J.G., Carter, D.J.D. and Larson, D.N. "High-throughput nanohole array based system to monitor multiple binding events in real time." *Analytical Chemistry* **80**, 2491–2498 (2008).
138. Im, H., Lesuffleur, A., Lindquist, N.C. and Oh, S.-H. "Plasmonic nanoholes in a multichannel microarray format for parallel kinetic assays and differential sensing." *Analytical Chemistry* **81**, 2854–2859 (2009).
139. Yang, J., Ji, J., Hogle, J.M. and Larson, D.N. "Multiplexed plasmonic sensing based on small-dimension nanohole arrays and intensity interrogation." *Biosensors & Bioelectronics* **24**, 2334–2338 (2009).
140. Yang, J., Ji, J., Hogle, J.M. and Larson, D.N. "Metallic nanohole arrays on fluoropolymer substrates as small label-free real-time bioprobes." *Nano Letters* **8**, 2718–2724 (2008).
141. Endo, T., Kerman, K., Nagatani, N., Hiepa, H.M., Kim, D.-K., Yonezawa, Y., Nakano, K. and Tamiya, E. "Multiple label-free detection of antigen-antibody reaction using localized surface plasmon resonance-based core-shell structured nanoparticle layer nanochip." *Analytical Chemistry* **78**, 6465–6475 (2006).
142. Piliarik, M., Šípová, H., Kvasnička, P., Galler, N., Krenn, J.R. and Homola, J. "High-resolution biosensor based on localized surface plasmons." *Optics Express* **20**, 672–680 (2011).
143. Proll, G., Steinle, L., Pröll, F., Kumpf, M., Moehrl, B., Mehlmann, M. and Gauglitz, G. "Potential of label-free detection in high-content-screening applications." *Journal of Chromatography. A* **1161**, 2–8 (2007).
144. Birkert, O. and Gauglitz, G. "Development of an assay for label-free high-throughput screening of thrombin inhibitors by use of reflectometric interference spectroscopy." *Analytical and Bioanalytical Chemistry* **372**, 141–147 (2002).
145. Ozkumur, E., Needham, J.W., Bergstein, D.A., Gonzalez, R., Cabodi, M., Gershoni, J.M., Goldberg, B.B. and Unlü, M.S. "Label-free and dynamic detection of biomolecular interactions for high-throughput microarray applications." *Proceedings of the National Academy of Sciences of the United States of America* **105**, 7988–7992 (2008).
146. Ozkumur, E., Yalçın, A., Cretich, M., Lopez, C.A., Bergstein, D.A., Goldberg, B.B., Chiari, M. and Unlü, M.S. "Quantification of DNA and protein adsorption by optical phase shift." *Biosensors & Bioelectronics* **25**, 167–172 (2009).
147. Ozkumur, E., Lopez, C. a, Yalçın, A., Connor, J.H., Chiari, M. and Unlü, M.S. "Spectral Reflectance Imaging for a Multiplexed, High-Throughput, Label-Free, and Dynamic Biosensing Platform." *IEEE Journal of Selected Topics in Quantum Electronics* **16**, 635–646 (2010).
148. Ozkumur, E., Ahn, S., Yalçın, A., Lopez, C.A., Cevik, E., Irani, R.J., DeLisi, C., Chiari, M. and Unlü, M.S. "Label-free microarray imaging for direct detection of DNA hybridization and single-nucleotide mismatches." *Biosensors & Bioelectronics* **25**, 1789–1795 (2010).
149. Daaboul, G.G., Vedula, R.S., Ahn, S., Lopez, C.A., Reddington, A., Ozkumur, E. and Unlü, M.S. "LED-based interferometric reflectance imaging sensor for quantitative dynamic monitoring of biomolecular interactions." *Biosensors & Bioelectronics* **26**, 2221–2227 (2011).
150. Ymeti, A. "Development of a multichannel integrated interferometer immunosensor." *Sensors and Actuators B: Chemical* **83**, 1–7 (2002).
151. Ymeti, A., Kanger, J.S., Greve, J., Besselink, G. a J., Lambeck, P.V., Wijn, R. and Heideman, R.G. "Integration of microfluidics with a four-channel integrated optical Young interferometer immunosensor." *Biosensors & Bioelectronics* **20**, 1417–1421 (2005).
152. Ymeti, A., Greve, J., Lambeck, P.V., Wink, T., van Hövell, S.W.F.M., Beumer, T. a M., Wijn, R.R., Heideman, R.G., Subramaniam, V. and Kanger, J.S. "Fast, ultrasensitive virus detection using a Young interferometer sensor." *Nano Letters* **7**, 394–397 (2007).
153. Petrou, P.S., Kitsara, M., Makarona, E., Raptis, I., Kakabakos, S.E., Stoffer, R., Jobst, G. and Misiakos, K. "Monolithically integrated biosensors based on Frequency-Resolved Mach-Zehnder Interferometers for multi-analyte determinations." *Engineering in Medicine and Biology Society (EMBC), 2010 Annual International Conference of the IEEE* 298–301 (2010). doi:10.1109/IEMBS.2010.5627478
154. Vollmer, F., Braun, D., Libchaber, A., Khoshshima, M., Teraoka, I. and Arnold, S. "Protein detection by optical shift of a resonant microcavity." *Applied Physics Letters* **80**, 4057–4059 (2002).
155. Ligler, F.S., Breimer, M., Golden, J.P., Nivens, D. a, Dodson, J.P., Green, T.M., Haders, D.P. and Sadik, O. a. "Integrating waveguide biosensor." *Analytical Chemistry* **74**, 713–719 (2002).
156. Vollmer, F., Arnold, S., Braun, D., Teraoka, I. and Libchaber, A. "Multiplexed DNA quantification by spectroscopic shift of two microsphere cavities." *Biophysical Journal* **85**, 1974–1979 (2003).
157. White, I.M., Oveys, H., Fan, X., Smith, T.L. and Zhang, J. "Integrated multiplexed biosensors based on liquid core optical ring resonators and antiresonant reflecting optical waveguides." *Applied Physics Letters* **89**, 191106–191106-3 (2006).
158. Washburn, A.L., Gunn, L.C. and Bailey, R.C. "Label-free quantitation of a cancer biomarker in complex media using silicon photonic microring resonators." *Analytical Chemistry* **81**, 9499–9506 (2009).
159. Washburn, A.L., Luchansky, M.S., Bowman, A.L. and Bailey, R.C. "Quantitative, label-free detection of five protein biomarkers using multiplexed arrays of silicon photonic microring resonators." *Analytical Chemistry* **82**, 69–72 (2010).

160. Iqbal, M., Gleeson, M.A., Spaugh, B., Tybor, F., Gunn, W.G., Hochberg, M., Baehr-Jones, T., Bailey, R.C. and Gunn, L.C. "Label-free biosensor arrays based on silicon ring resonators and high-speed optical scanning instrumentation." *Selected Topics in Quantum Electronics, IEEE Journal of* **16**, 654–661 (2010).
161. Carlborg, C.F., Gylfason, K.B., Kaźmierczak, A., Dortu, F., Bañuls Polo, M.J., Maqueira Catala, A., Kresbach, G.M., Sohlström, H., Moh, T., Vivien, L., Popplewell, J., Ronan, G., Barrios, C.A., Stemme, G. and van der Wijngaart, W. "A packaged optical slot-waveguide ring resonator sensor array for multiplex label-free assays in labs-on-chips." *Lab on a Chip* **10**, 281–290 (2010).
162. Jin, G., Jansson, R. and Arwin, H. "Imaging ellipsometry revisited: Developments for visualization of thin transparent layers on silicon substrates." *Review of Scientific Instruments* **67**, 2930–2936 (1996).
163. Jin, G., Tengvall, P., Lundström, I. and Arwin, H. "A biosensor concept based on imaging ellipsometry for visualization of biomolecular interactions." *Analytical Biochemistry* **232**, 69–72 (1995).
164. Cunningham, B., Li, P., Lin, B. and Pepper, J. "Colorimetric resonant reflection as a direct biochemical assay technique." *Sensors and Actuators B: Chemical* **81**, 316–328 (2002).
165. Cunningham, B., Qiu, J., Lin, B., Li, P. and Pepper, J. "A plastic colorimetric resonant optical biosensor for multiparallel detection of label-free biochemical interactions." *Proceedings of IEEE Sensors* **85**, 212–216 (2002).
166. Cunningham, B., Lin, B., Qiu, J., Li, P., Pepper, J. and Hugh, B. "A plastic colorimetric resonant optical biosensor for multiparallel detection of label-free biochemical interactions." *Sensors and Actuators B: Chemical* **85**, 219–226 (2002).
167. Yan, R., Mestas, S.P., Yuan, G., Safaisini, R., Dandy, D.S. and Lear, K.L. "Label-free silicon photonic biosensor system with integrated detector array." *Lab on a Chip* **9**, 2163–2168 (2009).
168. Choi, C.J. and Cunningham, B.T. "A 96-well microplate incorporating a replica molded microfluidic network integrated with photonic crystal biosensors for high throughput kinetic biomolecular interaction analysis." *Lab on a Chip* **7**, 550–556 (2007).
169. Mandal, S., Goddard, J.M. and Erickson, D. "A multiplexed optofluidic biomolecular sensor for low mass detection." *Lab on a Chip* **9**, 2924–2932 (2009).
170. Shamah, S.M. and Cunningham, B.T. "Label-free cell-based assays using photonic crystal optical biosensors." *The Analyst* **136**, 1090–1102 (2011).
171. Luchansky, M.S. and Bailey, R.C. "High-Q optical sensors for chemical and biological analysis." *Analytical Chemistry* **84**, 793–821 (2012).
172. St-Louis, P. "Status of point-of-care testing: promise, realities, and possibilities." *Clinical Biochemistry* **33**, 427–440 (2000).
173. Kodadek, T. "Protein microarrays: prospects and problems." *Chemistry & Biology* **8**, 105–115 (2001).
174. Wan, Y., Zheng, Z., Lu, Z., Liu, J. and Zhu, J. "Self-referenced sensing based on a waveguide-coupled surface plasmon resonance structure for background-free detection." *Sensors and Actuators B: Chemical* **162**, 35–42 (2012).
175. Abbas, A., Linman, M.J. and Cheng, Q. "New trends in instrumental design for surface plasmon resonance-based biosensors." *Biosensors & Bioelectronics* **26**, 1815–1824 (2011).
176. Regatos, D., Fariña, D., Calle, A., Cebollada, A., Sepúlveda, B., Armelles, G. and Lechuga, L.M. "Au/Fe/Au multilayer transducers for magneto-optic surface plasmon resonance sensing." *Journal of Applied Physics* **108**, 054502–054502-6 (2010).
177. Regatos, D., Sepúlveda, B., Fariña, D., Carrascosa, L.G. and Lechuga, L.M. "Suitable combination of noble/ferromagnetic metal multilayers for enhanced magneto-plasmonic biosensing." *Optics Express* **19**, 8336–8346 (2011).
178. Live, L.S., Murray-Méhot, M.-P. and Masson, J.-F. "Localized and Propagating Surface Plasmons in Gold Particles of Near-Micron Size." *The Journal of Physical Chemistry C* **113**, 40–44 (2009).
179. Live, L.S., Bolduc, O.R. and Masson, J. "Propagating surface plasmon resonance on microhole arrays." *Analytical Chemistry* **82**, 3780–3787 (2010).
180. Bolduc, O.R. and Masson, J. "Advances in surface plasmon resonance sensing with nanoparticles and thin films: nanomaterials, surface chemistry, and hybrid plasmonic techniques." *Analytical Chemistry* **83**, 8057–8062 (2011).
181. Kohl, J., Fireman, M. and O'Carroll, D. "Surface plasmon and photonic mode propagation in gold nanotubes with varying wall thickness." *Physical Review B* **84**, 1–8 (2011).
182. Aćimović, S.S., Kreuzer, M.P., González, M.U. and Quidant, R. "Plasmon near-field coupling in metal dimers as a step toward single-molecule sensing." *ACS Nano* **3**, 1231–1237 (2009).
183. Sípová, H., Zhang, S., Dudley, A.M., Galas, D., Wang, K. and Homola, J. "Surface plasmon resonance biosensor for rapid label-free detection of microribonucleic acid at sub-femtomole level." *Analytical Chemistry* **82**, 10110–10115 (2010).
184. Wijaya, E., Lenaerts, C., Maricot, S., Hastanin, J., Habraken, S., Vilcot, J.-P., Boukherroub, R. and Szunerits, S. "Surface plasmon resonance-based biosensors: From the development of different SPR structures to novel surface functionalization strategies." *Current Opinion in Solid State and Materials Science* **15**, 208–224 (2011).
185. Kastl, K.F., Lowe, C.R. and Norman, C.E. "Encoded and multiplexed surface plasmon resonance sensor platform." *Analytical Chemistry* **80**, 7862–7869 (2008).
186. Liu, Z., Bucknall, D.G. and Allen, M.G. "Inclined nanoimprinting lithography-based 3D nanofabrication." *Journal of Micromechanics and Microengineering* **21**, 065036 (2011).
187. Fu, J., Cao, Z. and Yobas, L. "Localized oblique-angle deposition: Ag nanorods on microstructured surfaces and their SERS characteristics." *Nanotechnology* **22**, 505302 (2011).

188. Dostert, K.-H., Alvarez, M., Koynov, K., Del Campo, A., Butt, H.-J. and Kreiter, M. "Near field guided chemical nanopatterning." *Langmuir* **28**, 3699–3703 (2012).
189. Jones, M.R., Osberg, K.D., Macfarlane, R.J., Langille, M.R. and Mirkin, C. a. "Templated techniques for the synthesis and assembly of plasmonic nanostructures." *Chemical Reviews* **111**, 3736–3827 (2011).
190. Tanabe, I. and Tatsuma, T. "Size- and Shape-Controlled Electrochemical Deposition of Metal Nanoparticles by Tapping Mode Atomic Force Microscopy." *The Journal of Physical Chemistry C* **116**, 3995–3999 (2012).
191. Satija, J., Sai, V. and Mukherji, S. "Dendrimers in biosensors: Concept and applications." *Journal of Materials Chemistry* **21**, 14367–14386 (2011).
192. Moreira, C.S., Neto, A.G.S.B., Lima, A.M.N., Thirstrup, C. and Neff, H. "Exchangeable low cost polymer biosensor chip for surface plasmon resonance spectroscopy." *Procedia Chemistry* **1**, 1479–1482 (2009).
193. Buijs, J. and Franklin, G.C. "SPR-MS in functional proteomics." *Briefings in Functional Genomics & Proteomics* **4**, 39–47 (2005).
194. Nedelkov, D. and Nelson, R.W. "Surface plasmon resonance mass spectrometry: recent progress and outlooks." *Trends in Biotechnology* **21**, 301–305 (2003).



Soumyo Mukherji did his B.Tech (Instrumentation Engineering) from Indian Institute of Technology Kharagpur, India, M.S. from Colorado State University (Fort Collins, USA) and PhD from University of North Carolina (Chapel Hill, USA). Currently he is a professor in the Department of Bio-

sciences and Bioengineering and the Head of the Centre for Research in Nanotechnology and Sciences at the Indian Institute of Technology Bombay. His research interests include micro and nano sensors for physical, chemical and biological applications as well as instrumentation systems for widescale deployment.



Nirmal Punjabi did his B.E. in Biomedical Engineering from Thadomal Shahani Engineering College, Mumbai, in 2009. Since then he is pursuing his M.Tech + PhD in field of biosensors from the Indian Institute of Technology, Bombay.

